

## Somatic mutations and T-cell clonality in patients with immunodeficiency

Paula Savola,<sup>1,2</sup> Timi Martelius,<sup>3</sup> Matti Kankainen,<sup>1,2,4,5</sup> Jani Huuhtanen,<sup>1,2</sup> Sofie Lundgren,<sup>1,2</sup> Yrjö Koski,<sup>1,2</sup> Samuli Eldfors,<sup>4</sup> Tiina Kelkka,<sup>1,2</sup> Mikko A.I. Keränen,<sup>1,2</sup> Pekka Ellonen,<sup>4</sup> Panu E. Kovanen,<sup>6</sup> Soili Kytölä,<sup>7</sup> Janna Saarela,<sup>4</sup> Harri Lähdesmäki,<sup>8</sup> Mikko R.J. Seppänen<sup>2,3,9</sup> and Satu Mustjoki<sup>1,2,10</sup>

<sup>1</sup>Hematology Research Unit Helsinki, University of Helsinki and Department of Hematology, HUS Helsinki University Hospital Comprehensive Cancer Center, Helsinki; <sup>2</sup>Translational Immunology Research Program, University of Helsinki, Helsinki; <sup>3</sup>Adult Immunodeficiency Unit, Infectious Diseases, Inflammation Center, University of Helsinki, HUS Helsinki University Hospital, Helsinki; <sup>4</sup>Institute for Molecular Medicine Finland (FIMM), HILIFE, University of Helsinki, Helsinki; <sup>5</sup>Medical and Clinical Genetics, University of Helsinki and HUS Helsinki University Hospital, Helsinki; <sup>6</sup>Department of Pathology, University of Helsinki and HUSLAB, HUS Helsinki University Hospital, Helsinki; <sup>7</sup>Laboratory of Genetics, HUSLAB, HUS Helsinki University Hospital, Helsinki; <sup>8</sup>Department of Computer Science, Aalto University School of Science, Espoo; <sup>9</sup>Rare Diseases Center and Pediatric Research Center, Children and Adolescents, University of Helsinki and HUS Helsinki University Hospital, Helsinki and <sup>10</sup>Department of Clinical Chemistry and Hematology, University of Helsinki, Helsinki, Finland

©2020 Ferrata Storti Foundation. This is an open-access paper. doi:10.3324/haematol.2019.220889

Received: March 14, 2019.

Accepted: December 18, 2019.

Pre-published: December 19, 2019.

Correspondence: SATU MUSTJOKI - satu.mustjoki@helsinki.fi

---

## Supplementary information

### **Somatic mutations and T-cell clonality in patients with immunodeficiency**

Paula Savola<sup>1,2</sup>, Timi Martelius<sup>3</sup>, Matti Kankainen<sup>1,2,4,5</sup>, Jani Huuhtanen<sup>1,2</sup>, Sofie Lundgren<sup>1,2</sup>, Yrjö Koski<sup>1,2</sup>, Samuli Eldfors<sup>4</sup>, Tiina Kelkka<sup>1,2</sup>, Mikko A.I. Keränen<sup>1,2</sup>, Pekka Ellonen<sup>4</sup>, Panu E. Kovanen<sup>6</sup>, Soili Kytölä<sup>7</sup>, Janna Saarela<sup>4</sup>, Harri Lähdesmäki<sup>8</sup>, Mikko R.J. Seppänen<sup>2,3,9</sup>, and Satu Mustjoki<sup>1,2,10</sup>

<sup>1</sup>Hematology Research Unit Helsinki, University of Helsinki and Department of Hematology, HUS Helsinki University Hospital Comprehensive Cancer Center, Helsinki, Finland; <sup>2</sup>Translational Immunology Research Program, University of Helsinki, Helsinki, Finland; <sup>3</sup>Adult Immunodeficiency Unit, Infectious Diseases, Inflammation Center, University of Helsinki, HUS Helsinki University Hospital, Helsinki, Finland; <sup>4</sup>Institute for Molecular Medicine Finland (FIMM), HILIFE, University of Helsinki, Helsinki, Finland; <sup>5</sup>Medical and Clinical Genetics, University of Helsinki and HUS Helsinki University Hospital, Helsinki, Finland; <sup>6</sup>Department of Pathology, University of Helsinki and HUSLAB, HUS Helsinki University Hospital, Helsinki, Finland; <sup>7</sup>Laboratory of Genetics, HUSLAB, HUS Helsinki University Hospital, Helsinki, Finland; <sup>8</sup>Department of Computer Science, Aalto University School of Science, Finland; <sup>9</sup>Rare Diseases Center and Pediatric Research Center, Children and Adolescents, University of Helsinki and HUS Helsinki University Hospital, Helsinki, Finland; <sup>10</sup>Department of Clinical Chemistry and Hematology, University of Helsinki, Helsinki, Finland

## Supplementary Methods

### Patients

We recruited 8 patients with late-onset CVID and 9 patients with other types of delayed-onset immunodeficiency or severe autoimmunity from the Helsinki University Hospital infectious disease clinic (Table 1). CVID patients were included in a previously described CVID cohort.<sup>1</sup> As healthy controls, we used blood donor buffy coat samples from the Red Cross Blood Service (Supplementary Table S1). This study was approved by local Ethics Committee, and the principles of Helsinki Declaration were followed. All patients signed informed consent.

Clinical manifestations of five patient cases have been previously described: patient 17 with biallelic germline mutation in *ADA2* gene (*CECRI*, p.Arg169Gln/p.Arg169Gln) and ADA2 deficiency,<sup>2</sup> patients 9-11 as germline gain-of-function mutations in *STAT3*,<sup>3</sup> and patient 12 as a case with compound immunodeficiency and 11q terminal deletion arr11q24.2q25 (126,074,297-134,927,114) x 1 (Jacobsen syndrome).<sup>4</sup>

### Sample preparation

Peripheral-blood EDTA samples were obtained from all patients. For patient 9, only archived bone-marrow mononuclear cells were available. Mononuclear cells were enriched from peripheral blood via Ficoll gradient centrifugation (Ficoll-Paque PLUS, GE Healthcare). CD4<sup>+</sup> and CD8<sup>+</sup> cells were purified via positive selection with magnetic beads (Miltenyi Biotec). Purity of sorted cells was controlled with flow cytometry with anti-CD45 (2D1, PerCP), anti-CD3 (SK7, FITC), anti-CD4 (SK3, APC), and anti-CD8 antibodies (SK1, PE-Cy7) (Beckton Dickinson). DNA was extracted with NucleSpin Tissue kit (Machery Nagel) according to manufacturer's instructions; however, the samples of patient 15 were extracted with Qiagen DNEasy Blood & Tissue kit (Qiagen). B-cell phenotypes were analyzed with flow cytometry in a clinical laboratory according to published guidelines.<sup>5,6</sup>

### T-cell receptor beta locus sequencing

*TCRB* sequencing was performed from CD8<sup>+</sup> and CD4<sup>+</sup> cells with the human *TCRB* immunoSEQ kit (Adaptive Biotechnologies) according to manufacturer's instructions.<sup>7,8</sup> The *TCRB* sequencing procedures have been described previously.<sup>8,9</sup> Healthy controls' CD4<sup>+</sup> and CD8<sup>+</sup> cells were also sequenced (n=27), and results were compared with the results of 7 CVID patients (pt.1-7). Only productive TCR sequences were taken into account in the analyses. ImmunoSEQ Analyzer software

(Adaptive Biotechnologies) and R version 3.4.2 and RStudio (version 1.1.383) were used for data analyses. The clonality metric was calculated as one minus Shannon entropy normalized by the logarithm of the number of productive TCR sequences.

To search for public TCR sequences, such as public pathogen-specific TCRs, we queried our TCR sequencing dataset on public TCRs that were included in the manually curated McPAS database, which includes approximately 9500 human TCR sequences.<sup>10</sup> For pathogen- and cancer-associated TCRs, only antigen-specific TCRs were queried (labels “1” and “2” in the McPAS database), but for autoimmune TCRs, all autoimmune-associated TCRs were included in the analyses. The pathogen-specific public TCRs comprised of TCRs targeting CMV, EBV, influenza, HIV, yellow fever virus, *Mycobacterium tuberculosis*, Herpes simplex 2 virus, and hepatitis C virus.

Physico-chemical similarities between TCRs were analyzed with a generic string kernel (GSKernel) algorithm,<sup>11</sup> which is designed for analysis of small peptides. The unsupervised clustering analysis of the TCR similarities was done with graph-theory based PhenoGraph.<sup>12</sup> The results were visualized with t-Distributed Stochastic Neighbor Embedding (t-SNE).<sup>13</sup> To focus on the most biologically meaningful TCRs and to minimize the amount of noise, we included only a subset of TCRs for the analyses:

1. Convergent TCRs that have more than 5 different clones OR convergent TCRs that make up at least 1% of the repertoire (“highly convergent”)
2. TCR clones that comprise at least 1% of all rearrangements (CD8+ cells) or 0.1% of all rearrangements (CD4+ cells) (“highly expanded”)

Also, these “highly convergent” and “expanded” clones were compared for their TCR amino-acid properties yielded by the “peptides” R package, which yields scores on the Cruciani *et al* properties (Polarity, Hydrophobicity, H-bonding),<sup>14</sup> GRAVY hydrophobicity index, and net charge.

### **Somatic variant detection: Sequencing library preparation**

To discover somatic variants that occur even at small variant allele frequencies, we designed a custom sequencing panel that comprised of the coding areas of 2533 genes, covering approximately 5.2 million base-pairs. The gene selection was based on the InnateDB database (<http://www.innatedb.ca/>),<sup>15-17</sup> but also other genes that were important in hematopoietic cells, adaptive immune responses, and autoimmunity were included (Supplementary Table S2). The target probes were designed with NimbleGen SeqCap EZ Developer system.

All immunodeficiency patient samples and 12/21 control samples were prepared for targeted sequencing with Kapa Hyper library preparation kit (Roche). Double-stranded genomic DNA (300-500ng) was fragmented with Covaris E220 evolution instrument (Covaris) to retrieve mean fragment size of 200 base-pairs. Sample libraries and enrichment were performed according to SeqCapEZ HyperCap Workflow User's Guide version 1.0 (Roche Nimblegen). SeqCap adapters and 9 cycles were used for pre-capture amplification. Four samples were multiplexed for capture using 1 ug of each library. Post-capture amplification included 10 cycles. Libraries were quantified with 2100 Bioanalyzer High Sensitivity Kit (Agilent Technologies).

For 9/21 control samples, ThruPLEX DNA-seq library preparation kit (Rubicon Genomics) was used. Double-stranded genomic DNA (100ng) was fragmented with Episonic Multi-Functional Bioprocessor 1100 (Epigenetik Group Inc.) to retrieve mean fragment size of 200 base-pairs. Sequencing libraries were prepared according to ThruPLEX DNA-seq library preparation kit protocol (Rubicon Genomics) with five amplification cycles. Libraries were quantified with LabChip GX (Caliper Life Sciences, Inc.). Eight samples (100ng DNA each) were pooled for hybridization and target capture, and targets were captured according to "Exome Capture of ThruPLEX Libraries with Roche NimbleGen SeqCap EZ Library" (Rubicon Genomics) and "NimbleGen SeqCap EZ Exome Library SR User's Guide" (Roche). Post-capture amplification was performed with 10 cycles. Quantification for sequencing was performed with 2100 Bioanalyzer High Sensitivity Kit (Agilent Technologies). All samples were sequenced with HiSeq2500 (Illumina) with HiSeq high output mode using v4 kits (Illumina), using 101-length paired-end reads.

### **Somatic variant detection: Sequencing data analysis**

Genome variants were called using a previously established Genome Analysis Toolkit (GATK) protocol.<sup>18</sup> Briefly, sequencing data was pre-processed with the Trimmomatic software,<sup>19</sup> and aligned to the GRCh38 genome with BWA-MEM.<sup>20</sup> The Picard toolset was used to mark PCR duplicates. Base recalibration was then performed with GATK BaseRecalibrator.<sup>21</sup> GATK IndelRealigner was used for local realignment near indels, and GATK CalculateContamination was used to estimate cross-sample contaminations. Somatic variants were identified using the MuTect2 toolset with default settings, using a panel of normals based on data from the 21 healthy control samples.<sup>22</sup> Finally, levels of 8-oxoguanine and deamination artifacts were estimated and variant calls resulting from sequencing artifacts filtered. Calling of variants relied on GATK version

3 tools and GATK resource files that were converted from GRCh37 to GRCh38 using CrossMap<sup>23</sup> and Ensembl chain files downloaded from Ensembl. GATK version 4 tools were used to estimate levels sequencing artifacts and cross-sample contamination.

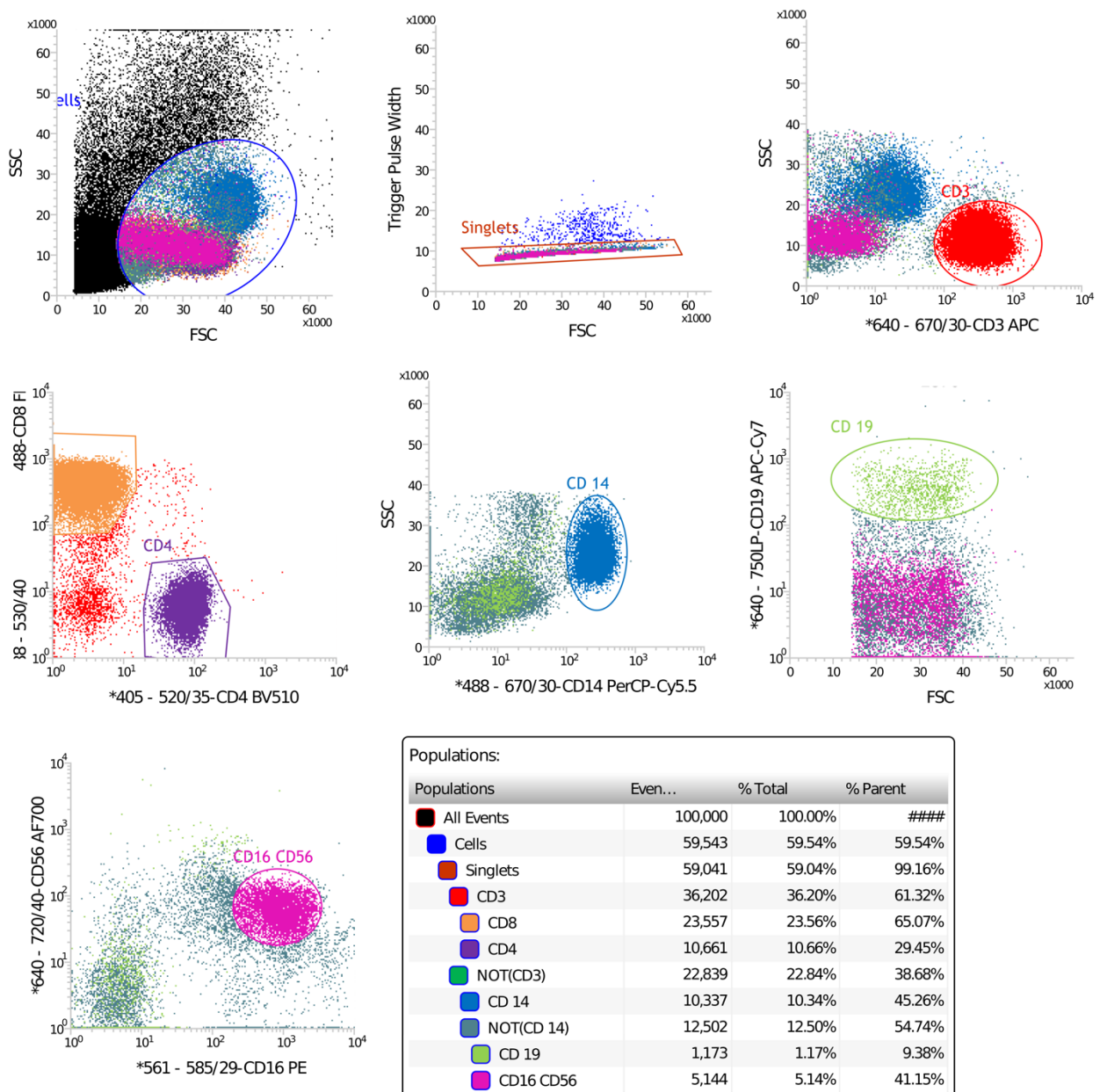
Filtering and annotation of variant calls was based on in-house scripts and Annovar.<sup>24</sup> Briefly, variant calls passing standard MuTect2 filters and with a quality of  $\geq 40$ , read depth of  $\geq 7$ ,  $\geq 1$  forward and reverse strand read, and strand orientation bias (SOR) of  $\leq 3$  for single-nucleotide alterations or  $\leq 1$  for indel alterations were accepted. False-positive variant calls were then further filtered by removing calls with a variant allele frequency (VAF) of  $\leq 1\%$ , calls with a VAF of 1-2% and supported by  $\leq 5$  Catalogue of Somatic Mutations in Cancer (COSMIC) hematopoietic tissue samples, and calls that were associated with a population frequency  $> 1\%$  in gnomAD exome ALL, gnomAD exome FIN, gnomAD exome NFE, esp6500, or 1000g collections. Intronic and inframe variant calls were also removed. For all downstream analyses except mutational signature analyses, only nonsynonymous and splice-site mutations were included. Finally, nonsynonymous and splice-site variants were inspected visually with Integrative Genomics Viewer (IGV) to ensure high quality of variants.

Somatic variants specific for CD4+ and CD8+ fractions were identified by performing a tumor-normal MuTect2 analysis between datasets in both directions. This procedure eliminates germline-derived variants. Variants that originate from hematopoietic progenitors (clonal hematopoiesis) and occurring in both CD4+ and CD8+ cells were in turn identified using MuTect2 tumor-only strategy and by searching for somatic calls mutually present in both fractions. To avoid false findings among these “clonal hematopoiesis -associated” variant calls, only variant calls associated with known clonal hematopoiesis -associated genes<sup>25-27</sup> and with a VAF of  $\geq 2\%$  in at least one fraction were accepted. Variants were also quality checked using IGV and indel calls were not allowed to be within 5 base-pairs of a homopolymer or repeat region.

Signaling pathways were annotated using the Reactome public database,<sup>28</sup> and gene functions were annotated using Gene Ontology (GO) Consortium database “biological process” terms (Supplementary Table S3).<sup>29,30</sup> Mutational signatures were identified from both non-coding mutations and mutations that alter protein amino-acid sequence with deconstructSigs with default parameters and cancer profiles downloaded from the COSMIC web site in 09/2017.<sup>31,32</sup> The variant filtering criteria for signature analyses were 2% VAF, at least 7 supporting reads, and variant calls in both reverse and forward strands.

## Flow-cytometry-mediated cell sorting

We performed cell sorting to extract multiple, pure cell fractions from four patient samples (patients 2, 13, 16, 17). Patients' mononuclear cells were stained with the following antibodies: CD3-APC (SK7), CD8-FITC (SK1), CD4-BV510 (SK3), CD19-APC-Cy7 (SJ25C1), CD56-AF700 (B159), CD16-PE (Leu11c), CD14-PerCP-Cy5.5 (M5E2). They were sorted into CD3+CD4+, CD3+CD8+, CD3<sup>neg</sup>CD19+, CD3<sup>neg</sup>CD14+ and CD56+CD16+ cell fractions by FACS Influx (Beckton Dickinson). DNA was extracted by Qiagen DNEasy Blood & Tissue kit (Qiagen) according to manufacturer's instructions. DNA samples were prepared for Amplicon sequencing as described below. However, the yield of the fraction containing NK cells was so small that NK cells were not sequenced. The gating strategy is shown in the figure below. The purity of sorted fractions was controlled and was nearly 100%.



### **Amplicon sequencing: confirmation of mutations with a multiplex panel**

To gain higher confidence in the low VAF somatic mutations we performed a validation experiment by designing primers to cover genomic loci of 41 positions (Supplementary Table S9). Of these positions, 17 positions were negative controls. These 17 positions did not include any variants in the immunogene panel sequencing in our patient samples but had COSMIC identifiers. All positions were covered by amplicon primers that were multiplexed into a single reaction; the primers were designed by Paragon Genomics (Hayward, CA, USA) as a CleanPlex Custom NGS panel. Thus, all 41 positions were sequenced from all samples. Library preparation was performed according to manufacturer's instructions and the samples were sequenced with MiSeq PE150 v2 flow cell.

The sequencing data analysis pipeline has been described in detail previously.<sup>33</sup> Final variant refining included the following steps:

1. Discarding all variants with a frequency ratio less than 0.9
2. The variant must be first identified in the immunogene panel, as described in previous sections. Alternatively, it could be a control variant instead.
3. The variant should be supported by 10 or more reads. The VAFs of screened variants ranged from 0.017-0.13 in immunopanel data. Thus, a coverage of over 200-300 would be required to call variants in the positions with high confidence. Three amplicons had insufficient coverage (20-252x, Supplementary Table S9; *TET2* Q591fs, *DNMT3A* D531N, *JAK2* V617F) and were judged to be low confidence.

### **Additional Amplicon sequencing for *STAT5B* and *KRAS* mutations**

In addition to the multiplexed Amplicon panel sequencing, we performed single amplicon sequencing for three mutations: *STAT5B* N418K, *STAT5B* T628S and *KRAS* T58I. Samples for *STAT5B* sequencing were prepared by flow-cytometry-mediated cell sorting. PBMNCs were stained with CD3 (APC, SK7), CD4 (PerCP, SK3), CD8 (Pe-Cy7, SK1), CD14 (Pacific Blue, MHCD1428) antibodies and a Vbeta antibody corresponding to the largest CD8+ clone in the patient (IO Test Vbeta Mark Kit, Beckman Coulter, PE and FITC fluorochromes). Cells were sorted with FACSARIA II (Beckton Dickinson) into CD3+CD4+, CD3+CD8+Vbeta+, CD3+CD8+Vbeta<sup>neg</sup>, CD3<sup>neg</sup>CD14+ and CD3<sup>neg</sup>CD14<sup>neg</sup> cell fractions with nearly 100% purity. Afterwards, DNA extraction followed with the NucleSpin Tissue kit (Machery Nagel) according to manufacturer's instructions.



Short amplicons were designed to cover the mutation of interest. Amplicons were amplified with a two-step PCR protocol. The first PCR was performed in a volume of 20 $\mu$ l containing  $\leq$ 10ng of sample DNA, 10 $\mu$ l of 2 $\times$  Phusion High-Fidelity PCR Master Mix (Thermo Fisher Scientific, Waltham, MA, USA) and 0.25 $\mu$ M of each locus-specific primer. *KRAS* locus-specific primers were prone to forming primer dimers so 10 $\mu$ l of water was added to the ready PCR reaction to increase the volume to 30 $\mu$ l and the products were purified once with Agencourt AMPure XP beads (Beckman Coulter, Brea, CA, USA).

The second PCR was performed using the amplified product from step 1 and index primers. DNA Engine Tetrad 2 (Bio-Rad Laboratories) or G-Storm GS4 (Somerton) thermal cyclers were used to cycle both PCR steps. 27 cycles were used for the first PCR and 8 for the second (Index PCR). The amplified samples were pooled and the pool was purified with Agencourt AMPure XP beads twice using 0.8x volume of beads compared to the sample pool volume. Agilent 2100 Bioanalyzer (Agilent Genomics, Santa Clara, CA, USA) was used to quantify amplification performance and yield of the purified sample pools. Sample pools were sequenced with Illumina MiSeq System using Illumina MiSeq Reagent Kit v3 600 cycles kit (Illumina, San Diego, CA, USA).

### **RNA sequencing**

To study if genes with somatic mutations are expressed in CD4<sup>+</sup> or CD8<sup>+</sup> cells, we utilized RNA sequencing from healthy controls' CD4<sup>+</sup> cells (n=3) and CD8<sup>+</sup> cells (n=5). RNA was extracted with miRNeasy kit including DNase I digestion (Qiagen) or NucleoSpin RNA II kit (Machery-Nagel) according to manufacturer's instructions. Total RNA (1-3 $\mu$ g) of cells was depleted from ribosomal RNA (Ribo-Zero, Epicentre). Ribodepleted and purified RNA (Nucleospin cleanup XS, Machery-Nagel) was converted to ds cDNA with the SuperScript Double-Stranded cDNA Synthesis Kit (Life Technologies), in all but two CD4<sup>+</sup> samples, in which the NEBNext mRNA Library Prep Master Mix Set for Illumina was used. Random hexamers (New England BioLabs) were used to prime the first strand synthesis reaction and SPRI beads (Agencourt AMPure XP, Beckman Coulter) for cDNA purification. Illumina-compatible Nextera Technology (Illumina) was used for preparation of RNA sequencing libraries, but instead of DNA, ds cDNA (60ng) was used as a template. Following the tagmentation reaction, fragmented cDNA was purified with SPRI beads. To add Illumina-specific bridge-PCR sites and enrich the library, limited-cycle PCR (5 cycles) was done according to instructions of Nextera system with minor modifications. For barcoded libraries, 50 X Nextera Adaptor 2 was replaced with Nextera Bar Codes kit adapters (Illumina) in the PCR setup. SPRI beads were employed to purify the PCR products. Library quality was evaluated with

Agilent Bioanalyzer (Agilent Technologies). Libraries were sequenced with Illumina HiSeq2000 or Illumina Genome Analyzer II to produce 100 base-pair paired-end reads.

RNA sequencing data was processed and aligned as has been previously described.<sup>18</sup> Reads were first trimmed with Trimmomatic and then mapped to the human GRCh38 reference (Ensembl 82) using STAR with the default 2-pass per-sample mapping settings.<sup>34</sup> Reads sorting and duplicate marking was performed with the Picard toolkit. FastQC and RNA-SeQC were used for quality control analysis. Mapped reads were assigned to gene features (Ensembl v82) using FeatureCounts.<sup>35</sup> Multi-mapping reads and assignment of a read to more than one overlapping feature were allowed. Read counts were normalized with the Trimmed Mean of M-values (TMM) method with edgeR with default parameters,<sup>36</sup> and transformed to  $\log_2$  values for graphing.

### **Statistical analyses**

Variant calling procedures are described in the “Somatic variant detection” -section. Statistical analyses were performed using GraphPad Prism v.6 (GraphPad Software) and R version 3.4.2 ([www.r-project.org](http://www.r-project.org)). Data were inspected for normality both graphically and with Shapiro-Wilk tests, but due to small sample size and/or data skewing, mostly nonparametric statistical tests were employed. Statistical tests included Spearman correlation, t-test, Mann-Whitney test, Kruskal-Wallis test, and Dunn’s multiple comparisons tests. Benjamini-Hochberg correction for multiple testing was used when analyzing V-family and J-gene usage.

**Supplementary Tables.**

**Supplementary Table S1. Healthy controls used in the study.**

Sample	Disease	Sex	Age	TCRB sequencing?	Immunogene panel sequencing?
HC1	HC	F	58	yes	yes
HC2	HC	M	58	yes	yes
HC13	HC	F	66	yes	yes
HC7	HC	M	48	yes	yes
HC8	HC	F	57	yes	yes
HC9	HC	F	56	yes	yes
HC10	HC	F	47	yes	yes
HC11	HC	M	48	yes	yes
HC12	HC	F	21	yes	yes
HC4	HC	F	44	yes	yes
HC5	HC	M	55	yes	yes
HC6	HC	M	52	yes	yes
HC3	HC	F	65	yes	yes
HC14	HC	F	63	yes	yes
HC15	HC	M	63	yes	yes
HC16	HC	F	65	yes	yes
HC17	HC	M	64	yes	yes
HC18	HC	F	65	yes	yes
HC19	HC	M	64	yes	yes
HC20	HC	F	63	yes	yes
HC21	HC	M	64	no	yes
HC22	HC	M	61	yes	no
HC23	HC	F	50	yes	no
HC27	HC	M	60	yes	no
HC28	HC	M	43	yes	no
HC26	HC	M	70	yes	no
HC24	HC	F	50	yes	no
HC25	HC	F	62	yes	no

Healthy controls used in TCRB and immunogene panel sequencing. Both CD4+ and CD8+ cells were sequenced. The median age for controls in TCRB sequencing was 58 (interquartile range 50-64), and the mean 56.2 (95% confidence interval 52.2-60.3) The median age for controls immunogene panel was 58 (interquartile range 50-64) and the mean 56.5 (95% confidence interval 51.6-61.3).















CTSC	ENSG00000109861	MAPK1	ENSG00000100030	STIM1	ENSG00000167323	MPO	ENSG00000005381
CTSD	ENSG00000117984	MAPK10	ENSG00000109339	STK11	ENSG00000118046	MPZL3	ENSG00000160588
CTSF	ENSG00000174080	MAPK11	ENSG00000185386	STK3	ENSG00000104375	MR1	ENSG00000153029
CTSG	ENSG00000100448	MAPK12	ENSG00000188130	STK4	ENSG00000101109	TLR3	ENSG00000164342
CTSH	ENSG00000103811	MAPK13	ENSG00000156711	STMN1	ENSG00000117632	TLR4	ENSG00000136869
CTSK	ENSG00000143387	MAPK14	ENSG00000112062	STRADA	ENSG00000266173	TLR5	ENSG00000187554
CTSL	ENSG00000135047	MAPK3	ENSG00000102882	STUB1	ENSG00000103266	TLR6	ENSG00000174130
CTSO	ENSG00000256043	MAPK6	ENSG00000069956	STX11	ENSG00000135604	TLR7	ENSG00000196664
CTSS	ENSG00000163131	MAPK7	ENSG00000166484	STXBP2	ENSG00000076944	TLR8	ENSG00000101916
CTSV	ENSG00000136943	MAPK8	ENSG00000107643	SUCNR1	ENSG00000198829	TLR9	ENSG00000239732
CTSW	ENSG00000172543	MAPK8IP1	ENSG00000121653	SUGT1	ENSG00000165416	TMC6	ENSG00000141524
CTSZ	ENSG00000101160	MAPK8IP2	ENSG00000008735	SUOX	ENSG00000139531	TMC8	ENSG00000167895
CUL7	ENSG00000044090	MAPK8IP3	ENSG00000138834	SUZ12	ENSG00000178691	TMED7	ENSG00000134970
CUX1	ENSG00000257923	MAPK9	ENSG00000050748	SWAP70	ENSG00000133789	TMEM126A	ENSG00000171202
CX3CL1	ENSG00000006210	MAPKAPK2	ENSG00000162889	SYDE2	ENSG00000097096	TMEM173	ENSG00000184584
CX3CR1	ENSG00000168329	MAPKAPK3	ENSG00000114738	SYK	ENSG00000165025	TMEM220	ENSG00000187824
CXCL1	ENSG00000163739	MAPKAPK5	ENSG00000089022	SYNGR1	ENSG00000100321	TMEM30A	ENSG00000112697
CXCL10	ENSG00000169245	MAPT	ENSG00000186868	SYP	ENSG00000102003	TMIGD2	ENSG00000167664
CXCL11	ENSG00000169248	MARCH5	ENSG00000198060	TAB1	ENSG00000100324	TNF	ENSG00000232810
CXCL12	ENSG00000107562	MARCO	ENSG00000019169	TAB2	ENSG00000055208	TNFAIP3	ENSG00000118503
CXCL13	ENSG00000156234	MASP1	ENSG00000127241	TAB3	ENSG00000157625	TNFAIP8L2	ENSG00000163154
CXCL14	ENSG00000145824	MASP2	ENSG00000009724	TACR1	ENSG00000115353	TNFRSF10A	ENSG00000104689
CXCL16	ENSG00000161921	MAVS	ENSG00000088888	TAGAP	ENSG00000164691	TNFRSF10B	ENSG00000120889
CXCL2	ENSG00000081041	MAX	ENSG00000125952	TAL1	ENSG00000162367	TNFRSF10C	ENSG00000173535
CXCL3	ENSG00000163734	MB21D1	ENSG00000164430	TANK	ENSG00000136560	TNFRSF10D	ENSG00000173530
CXCL5	ENSG00000163735	MBL2	ENSG00000165471	TAOK1	ENSG00000160551	TNFRSF11A	ENSG00000141655
CXCL6	ENSG00000124875	MBP	ENSG00000197971	TAOK2	ENSG00000149930	TNFRSF12A	ENSG00000006637
CXCL9	ENSG00000138755	MBTPS1	ENSG00000140943	TAOK3	ENSG00000135090	TNFRSF13B	ENSG00000240505
CXCR1	ENSG00000163464	MBTPS2	ENSG00000012174	TAP1	ENSG00000168394	TNFRSF13C	ENSG00000159958
CXCR2	ENSG00000180871	MCAM	ENSG00000076706	TAP2	ENSG00000204267	TNFRSF14	ENSG00000157873
CXCR3	ENSG00000186810	MCL1	ENSG00000143384	TAPBP	ENSG000000231925	TNFRSF17	ENSG00000048462
CXCR4	ENSG00000121966	MCM10	ENSG00000065328	TAX1BP1	ENSG00000106052	TNFRSF18	ENSG00000186891
CXCR5	ENSG00000160683	MCM4	ENSG00000104738	TAZ	ENSG00000102125	TNFRSF1A	ENSG00000067182
CXCR6	ENSG00000172215	MDC1	ENSG00000137337	TBK1	ENSG00000183735	TNFRSF1B	ENSG00000121837
CYBA	ENSG00000051523	MDM2	ENSG00000135679	TBKBP1	ENSG00000198933	TNFRSF25	ENSG00000215788
CYBB	ENSG00000165168	MECOM	ENSG00000085276	TBL1XR1	ENSG00000177565	TNFRSF4	ENSG00000186827
CYCS	ENSG00000172115	MED1	ENSG00000125686	TBX1	ENSG00000184058	TNFRSF8	ENSG00000120949
CYLD	ENSG00000083799	MED12	ENSG00000184634	TBX21	ENSG00000073861	TNFRSF9	ENSG00000049249
CYP24A1	ENSG00000019186	MEF2B	ENSG00000213999	TCEB1	ENSG00000154582	TNFSF10	ENSG00000121858
CYSLTR1	ENSG00000173198	MEF2C	ENSG00000081189	TCEB2	ENSG00000103363	TNFSF11	ENSG00000120659
CYTIP	ENSG00000115165	MEFV	ENSG00000103313	TCF3	ENSG00000071564	TNFSF12	ENSG00000239697
CYTL1	ENSG00000170891	MERTK	ENSG00000153208	TCF4	ENSG00000019628	TNFSF13	ENSG00000161955
DAB2IP	ENSG00000136848	MFF	ENSG00000168958	TCF7	ENSG00000081059	TNFSF13B	ENSG00000102524
DAG1	ENSG00000173402	MFGE8	ENSG00000140545	TCIRG1	ENSG00000110719	TNFSF14	ENSG00000125735
DAGLB	ENSG00000164535	MFI2	ENSG00000163975	TCL1A	ENSG00000100721	TNFSF15	ENSG00000181634
DAPK1-IT1	ENSG00000236709	MFN1	ENSG00000171109	TCL1B	ENSG00000213231	TNFSF4	ENSG00000117586
DAXX	ENSG00000204209	MFN2	ENSG00000116688	TCN2	ENSG00000185339	TNFSF8	ENSG00000106952
DCD	ENSG00000161634	MICA	ENSG00000204520	TDP2	ENSG00000111802	TNFSF9	ENSG00000125657
DCHS1	ENSG00000166341	MICB	ENSG00000204516	TEC	ENSG00000135605	TNIP1	ENSG00000145901
DCLRE1C	ENSG00000152457	MID1	ENSG00000101871	TECPR1	ENSG00000205356		
DCN	ENSG00000011465	MID2	ENSG00000080561	TEK	ENSG00000120156		
DDAH1	ENSG00000153904	MIF	ENSG00000240972	TENM3	ENSG00000218336		
DDI1	ENSG00000170967	MINOS1-NBL1/NBL1	ENSG00000158747	TERC	ENSG00000270141		
DDIT3	ENSG00000175197	MIR107	ENSG00000198997	TERF1	ENSG00000147601		
DDIT4	ENSG00000168209	MIR10A	ENSG00000274592	TERF2	ENSG00000132604		
DDR1	ENSG00000204580	MIR10B	ENSG00000207744	TERT	ENSG00000164362		
DDX1	ENSG00000079785	MIR1204	ENSG00000275264	TET1	ENSG00000138336		
DDX21	ENSG00000165732	MIR1208	ENSG00000221261	TET2	ENSG00000168769		
DDX3X	ENSG00000215301	MIR122	ENSG00000207778	TEX41	ENSG00000226674		
DDX41	ENSG00000183258	MIR124-1	ENSG00000275677	TFAP2A	ENSG00000137203		
DDX58	ENSG00000107201	MIR125B1	ENSG00000207971	TFPI	ENSG00000003436		
DEFA1	ENSG00000206047	MIR125B2	ENSG00000207863	TFR2	ENSG00000106327		
DEFA3	ENSG00000239839	MIR126	ENSG00000199161	TFRC	ENSG00000072274		
DEFA4	ENSG00000164821	MIR1275	ENSG00000221697	TGFB1	ENSG00000105329		
DEFA5	ENSG00000164816	MIR132	ENSG00000267200	TGFB2	ENSG00000092969		
DEFA6	ENSG00000164822	MIR133A1	ENSG00000276792	TGFB3	ENSG00000119699		
DEFB1	ENSG00000164825	MIR135B	ENSG00000199059	TGFBI	ENSG00000120708		
DEFB103A	ENSG00000176797	MIR141	ENSG00000207708	TGFBR1	ENSG00000106799		
DEFB103B	ENSG00000177243	MIR145	ENSG00000276365	TGFBR2	ENSG00000163513		
DEFB105A	ENSG00000186562	MIR146A	ENSG00000277727	TGFBR3	ENSG00000069702		
DEFB106A	ENSG00000186579	MIR149	ENSG00000207611	TGM2	ENSG00000198959		
DEFB119	ENSG00000180483	MIR15B	ENSG00000207779	THBD	ENSG00000178726		
DEFB123	ENSG00000180424	MIR16-1	ENSG00000208006	THBS1	ENSG00000137801		
DEFB4A	ENSG00000171711	MIR16-2	ENSG00000198987	THPO	ENSG00000090534		
DHCR24	ENSG00000116133	MIR181A2	ENSG00000207595	THRB	ENSG00000151090		
DHX36	ENSG00000174953	MIR187	ENSG00000207797	THY1	ENSG00000154096		
DHX58	ENSG00000108771	MIR200C	ENSG00000207713	TIAM1	ENSG00000156299		
DHX9	ENSG00000135829	MIR208B	ENSG00000215991	TICAM1	ENSG00000127666		
DICER1	ENSG00000100697	MIR21	ENSG00000199004	TICAM2	ENSG00000243414		
DIDO1	ENSG00000101191	MIR212	ENSG00000267195	TIMMDC1	ENSG00000113845		
DIS3	ENSG00000083520	MIR223	ENSG00000207939	TIMP1	ENSG00000102265		
DKC1	ENSG00000130826	MIR23A	ENSG00000207980	TINF2	ENSG00000092330		
DKKL1	ENSG00000104901	MIR23B	ENSG00000207563	TIRAP	ENSG00000150455		
DLG1	ENSG00000075711	MIR302B	ENSG00000274389	TKTL2	ENSG00000151005		
DLK1	ENSG00000185559	MIR3148	ENSG00000264788	TLN1	ENSG00000137076		
DMBT1	ENSG00000187908	MIR372	ENSG00000199095	TLR1	ENSG00000174125		
DNM1L	ENSG00000087470	MIR373	ENSG00000199143	TLR10	ENSG00000174123		
DNMT3A	ENSG00000119772	MIR497	ENSG00000273895	TLR2	ENSG00000137462		

Coding exons of listed genes were included in the custom sequencing panel. The table shows the genes and Ensembl Gene IDs for each sequenced gene.

**Supplementary Table S3. GO terms for gene annotations.**

Lymphocyte functions		Cell proliferation		Inflammation	
GO:0031295	GO:2001185	GO:0008283	GO:0042104	GO:0006925	
GO:0030217	GO:2000456	GO:0046316	GO:0042130	GO:0006954	
GO:0045058	GO:2000457	GO:0097325	GO:0003249	GO:1900225	
GO:0045066	GO:2000452	GO:1990705	GO:2000090	GO:1900227	
GO:0045065	GO:2000451	GO:0003263	GO:1905938	GO:1900226	
GO:0045062	GO:2000450	GO:0035988	GO:1905937	GO:1900016	
GO:0045061	GO:2000449	GO:0033687	GO:0060502	GO:1900015	
GO:0043029	GO:2000329	GO:0007405	GO:0060916	GO:1900017	
GO:0043316	GO:2000330	GO:0046651	GO:0035739	GO:0035492	
GO:0043379	GO:2000570	GO:0002941	GO:0035736	GO:0035491	
GO:0043368	GO:2000555	GO:0002158	GO:0035740	GO:0035490	
GO:0043383	GO:2000554	GO:0070661	GO:0060722	GO:0044546	
GO:0070489	GO:2000553	GO:0072574	GO:0033091	GO:0071646	
GO:0070231	GO:2000552	GO:0061517	GO:0033083	GO:0071647	
GO:0042093	GO:2000556	GO:0061516	GO:0033080	GO:0071648	
GO:0042098	GO:2000551	GO:0035172	GO:0033087	GO:0071642	
GO:0042110	GO:2000566	GO:0048144	GO:1902462	GO:0071640	
GO:0035709	GO:2000565	GO:0051450	GO:1902460	GO:0071641	
GO:0035704	GO:2000564	GO:0070341	GO:1902461	GO:0071607	
GO:0035683	GO:2000563	GO:0070343	GO:0032945	GO:0071608	
GO:0035685	GO:2000562	GO:0070342	GO:0032946	GO:0002861	
GO:0035684	GO:2000561	GO:0042100	GO:0032817	GO:0002862	
GO:0033079	GO:2000515	GO:0097360	GO:0032818	GO:0002863	
GO:0033078	GO:2000514	GO:0042098	GO:0032819	GO:0002864	
GO:0072678	GO:2000519	GO:0042127	GO:0071863	GO:0002865	
GO:0072683	GO:2000518	GO:0097166	GO:0046646	GO:0002866	
GO:0002870	GO:2000516	GO:0097168	GO:0046640	GO:0002874	
GO:0002572	GO:2000321	GO:1990654	GO:1901383	GO:0002875	
GO:0002517	GO:2000328	GO:1990739	GO:1901382	GO:0002876	
GO:0002456	GO:2000320	GO:1990863	GO:1901384	GO:0002877	
GO:0120117	GO:0050862	GO:1990922	GO:0071338	GO:0002878	
GO:0002360	GO:0050860	GO:0021534	GO:0071336	GO:0002879	
GO:0002369	GO:0052156	GO:0060720	GO:0071337	GO:0002880	
GO:0010818	GO:0090721	GO:0033079	GO:0002053	GO:0002881	
GO:0050798	GO:0090717	GO:0032943	GO:0002322	GO:0002882	
GO:0061485	GO:0002291	GO:0044565	GO:0002309	GO:0002673	
GO:0051132	GO:2001188	GO:0071425	GO:0070667	GO:0002674	
GO:0001913	GO:2001189	GO:0071335	GO:0070668	GO:0002675	
GO:0001866	GO:2001190	GO:0002174	GO:0033599	GO:0002676	
GO:0001865	GO:0043369	GO:0002176	GO:0072301	GO:0002677	
GO:0001777	GO:0032829	GO:0002358	GO:0072203	GO:0002678	
GO:1990656	GO:0032830	GO:0070662	GO:0072201	GO:0002523	
GO:0072735	GO:0032831	GO:0072343	GO:0072198	GO:0002525	
GO:0032292	GO:0032832	GO:0072137	GO:0072126	GO:0002526	
GO:0035398	GO:0002841	GO:0072135	GO:0072124	GO:0002527	
GO:0045059	GO:0002842	GO:0072122	GO:0072125	GO:0002528	
GO:0045064	GO:0002852	GO:0072123	GO:0072111	GO:0002532	
GO:0045063	GO:0002853	GO:0072110	GO:0072575	GO:0002533	
GO:0045068	GO:0002854	GO:0072089	GO:1904935	GO:0002534	
GO:0045067	GO:0002571	GO:0033278	GO:1904934	GO:0002535	
GO:0045060	GO:0002362	GO:0033002	GO:1904933	GO:0002536	
GO:0045580	GO:0002302	GO:0101023	GO:1905315	GO:0002537	
GO:0042129	GO:0002294	GO:0022034	GO:1905564	GO:0002538	
GO:0042492	GO:0002298	GO:0022022	GO:1905563	GO:0002539	
GO:0035707	GO:1905400	GO:0061518	GO:1905562	GO:0002540	
GO:0035712	GO:1905404	GO:0021928	GO:0022019	GO:0002541	
GO:0035711	GO:1905403	GO:0021929	GO:1904699	GO:0002544	
GO:0035706	GO:1905402	GO:0021926	GO:1904698	GO:0002545	
GO:0035705	GO:1905401	GO:0021846	GO:0021992	GO:0002437	
GO:0035699	GO:1905399	GO:0048659	GO:0021923	GO:0002438	
GO:0035688	GO:2001191	GO:0010463	GO:0021931	GO:0002439	
GO:0035687	GO:2001192	GO:0050798	GO:0021924	GO:0002441	
GO:0072736	GO:2001193	GO:0061485	GO:0021936	GO:0002442	
GO:0033077	GO:2000454	GO:0060038	GO:2001109	GO:0002349	
GO:1902482	GO:2000453	GO:0060011	GO:2001110	GO:0002351	
GO:1902483	GO:0052295	GO:0036093	GO:2001111	GO:0002391	
GO:0046630	GO:0052085	GO:0061351	GO:1904441	GO:0002393	
GO:0046629	GO:0090719	GO:0050674	GO:2000793	GO:0002232	
GO:0046633	GO:0032834	GO:0050673	GO:2000648	GO:0002246	
GO:0046631	GO:0032833	GO:0001935	GO:2000647	GO:0002247	
GO:0046632	GO:0052280	GO:0001866	GO:1902033	GO:0002248	
GO:0002770	GO:0072679	GO:0001834	GO:1902034	GO:0002269	
GO:0002680	GO:0071594	GO:0001787	GO:1902035	GO:1904597	
GO:0002667	GO:0070242	GO:0001777	GO:2000179	GO:1904596	
GO:0002512	GO:0070243	GO:0014009	GO:2000178	GO:1904598	
GO:0002458	GO:0042092	GO:0014010	GO:2000177	GO:0050727	
GO:0002364	GO:0072680	GO:0014856	GO:2000103	GO:0050729	
GO:0002295	GO:0072681	GO:0014855	GO:2000102	GO:0050728	
GO:0033371	GO:0071610	GO:0110021	GO:2000101	GO:0052259	
GO:0072539	GO:2000412	GO:0070444	GO:2000256	GO:0052256	
GO:2000407	GO:2000411	GO:0003264	GO:2000255	GO:0052260	
GO:2000404	GO:2000410	GO:003206	GO:2000254	GO:0052032	
GO:2000523	GO:2000413	GO:0048145	GO:2000231	GO:0052036	
GO:0010819	GO:2000400	GO:0010837	GO:2000230	GO:0052035	
GO:0050852	GO:2000399	GO:0090289	GO:2000229	GO:0060265	
GO:0050863	GO:2000398	GO:1904073	GO:0048662	GO:0060264	
GO:0061470	GO:0098915	GO:1904195	GO:0048661	GO:0060266	
GO:0001768	GO:0002325	GO:0030888	GO:0048660	GO:1904784	
GO:0036371	GO:0031294	GO:0070344	GO:0010456	GO:0090594	
GO:0046006	GO:0043366	GO:0042129	GO:0010626	GO:0106016	
GO:0046007	GO:0002461	GO:1990789	GO:0010625	GO:0106014	
GO:0046013	GO:0002437	GO:1990874	GO:0061469	GO:0106015	
GO:0046014	GO:0050851	GO:1905936	GO:0060045	GO:0006953	
GO:0006924	GO:1905024	GO:0035726	GO:0060044	GO:0031960	
GO:1903903	GO:0019724	GO:0060721	GO:0060043	GO:0006663	
GO:0045591	GO:0097026	GO:0032944	GO:0060253	GO:0030851	
GO:0045590	GO:0002348	GO:0044342	GO:0060252	GO:0018910	
GO:0045589	GO:0002350	GO:0071838	GO:1904705	GO:0043312	
GO:0045581	GO:0071652	GO:0046630	GO:1904898	GO:0070400	
GO:0045583	GO:0071609	GO:0046633	GO:1904897	GO:0097701	
GO:0045582	GO:2000415	GO:0002359	GO:1904899	GO:0042222	
GO:0045585	GO:2000414	GO:0070666	GO:0061323	GO:0097388	
GO:0045584	GO:0036399	GO:0033598	GO:0061325	GO:0042033	
GO:0045586	GO:0050854	GO:0072263	GO:0061209	GO:1990772	
GO:0043318	GO:0001806	GO:0072091	GO:0050677	GO:1990774	

GO:0043317	GO:0060307	GO:0008284	GO:0050676	GO:0042533
GO:0043319	GO:1905026	GO:0008285	GO:0050679	GO:0042534
GO:0043374	GO:1905025	GO:0022018	GO:0050680	GO:0042535
GO:0043367	GO:0097048	GO:0022012	GO:0039015	GO:0042536
GO:0043381	GO:0097029	GO:0022013	GO:0090095	GO:0042537
GO:0043380	GO:0097028	GO:0022020	GO:0051141	GO:0150076
GO:0043382	GO:0044565	GO:0022021	GO:0051142	GO:0034651
GO:0070238	GO:0002473	GO:1904697	GO:0051140	GO:0034650
GO:0070233	GO:0071649	GO:0021930	GO:0001938	GO:0071644
GO:0070232	GO:0071653	GO:0021925	GO:0001937	GO:0071645
GO:0070234	GO:0071654	GO:0010464	GO:0014011	GO:0071643
GO:0042102	GO:0072615	GO:0010624	GO:0014842	GO:0071606
GO:0042103	GO:0045222	GO:0060251	GO:0014859	GO:0046469
GO:0042104	GO:0035781	GO:0061270	GO:0014858	GO:0071385
GO:0042130	GO:0035780	GO:0050675	GO:0014857	GO:0071384
GO:0042722	GO:0050858	GO:0050678	GO:0003420	GO:0002558
GO:0035710	GO:0050857	GO:0001936	GO:0003265	GO:0002559
GO:0035739	GO:1990922	GO:0001833	GO:0003266	GO:0002524
GO:0035745	GO:0070266	GO:0014841	GO:0014844	GO:0002432
GO:0035744	GO:0071650	GO:0003419	GO:1901723	GO:0002445
GO:0035740	GO:0071651	GO:1902731	GO:1901722	GO:0016068
GO:0035783	GO:0002460	GO:1902732	GO:1901724	GO:0008211
GO:0035697	GO:1904837	GO:0035207	GO:1901963	GO:0072538
GO:1902232	GO:1904863	GO:0035208	GO:1901964	GO:1903492
GO:0031153	GO:0045210	GO:0048146	GO:0003250	GO:0050752
GO:0033090	GO:0035724	GO:0048147	GO:0003251	GO:0050751
GO:0033091	GO:0002569	GO:0010839	GO:0003252	GO:0050754
GO:0033082	GO:0002432	GO:0010838	GO:0003295	GO:0050753
GO:0033083	GO:0008626	GO:0090290	GO:2000092	GO:0050756
GO:0033080	GO:0048538	GO:0090291	GO:2000091	GO:0050755
GO:0033081	GO:0070244	GO:1904002	GO:0060501	GO:0050701
GO:0033086	GO:0070245	GO:1904003	GO:0060505	GO:0039573
GO:0033087	GO:1904865	GO:1904004	GO:0060517	GO:0051468
GO:0046646	GO:1904864	GO:1904075	GO:0060768	GO:0051384
GO:0046643	GO:0090737	GO:1904074	GO:0060767	GO:0001812
GO:0046640	GO:0001771	GO:1904196	GO:0060782	GO:0001811
GO:0046634	GO:0097720	GO:1904197	GO:0060781	GO:0001810
GO:0046637	GO:0070236	GO:0046006	GO:0060784	GO:0001809
GO:0002849	GO:0070239	GO:0046007	GO:0035742	GO:0001808
GO:0002709	GO:0070240	GO:0046013	GO:0035741	GO:0001807
GO:0002710	GO:0070241	GO:0046014	GO:0060750	GO:0001806
GO:0002711	GO:0070235	GO:0030889	GO:0060723	GO:0001805
GO:0002724	GO:0035397	GO:0030890	GO:0060650	GO:0001804
GO:0002725	GO:0035399	GO:0070347	GO:0060664	GO:0001803
GO:0002726	GO:0035743	GO:0070346	GO:0033601	GO:0001802
GO:0002664	GO:0035742	GO:0070349	GO:0033600	GO:0001801
GO:0002665	GO:0035741	GO:0070348	GO:0033092	GO:0001800
GO:0002666	GO:0035698	GO:0070350	GO:0033084	GO:0001799
GO:0002668	GO:1902233	GO:0070352	GO:0033088	GO:0001798
GO:0002669	GO:1902234	GO:0070351	GO:1902723	GO:0001797
GO:0002568	GO:0033092	GO:0070345	GO:1902724	GO:0001796
GO:0002457	GO:0033084	GO:0042102	GO:1902833	GO:0001795
GO:0002411	GO:0033085	GO:0042103	GO:1902832	GO:0001794
GO:0002363	GO:0033088	GO:2000080	GO:0032820	
GO:0002365	GO:0033089	GO:0060504	GO:0044340	
GO:0002304	GO:0046647	GO:0060770	GO:0071864	
GO:0002309	GO:0046644	GO:0060769	GO:0046647	
GO:0002286	GO:0046645	GO:0060651	GO:0046648	
GO:0002292	GO:0046648	GO:0035604	GO:0046642	
GO:0002296	GO:0046642	GO:1902727	GO:0046641	
GO:0002297	GO:0046641	GO:1902728	GO:0002043	
GO:0002299	GO:0046635	GO:0032821	GO:0002310	
GO:0045623	GO:0046636	GO:0032822	GO:0002311	
GO:0045624	GO:0046639	GO:0044343	GO:0002324	
GO:0045622	GO:0046638	GO:1903588	GO:0002289	
GO:0045628	GO:0002840	GO:1903589	GO:0072042	
GO:0045625	GO:0002846	GO:1903587	GO:0072302	
GO:0033374	GO:0002847	GO:0021922	GO:0072303	
GO:0033375	GO:0002848	GO:0021939	GO:0072200	
GO:0072540	GO:0002850	GO:0021938	GO:0072261	
GO:2000455	GO:0002851	GO:0038091	GO:0072262	
GO:2000409	GO:0002681	GO:0061324	GO:0072199	
GO:2000408	GO:0002625	GO:0061315	GO:0072138	
GO:2000406	GO:0002626	GO:0090256	GO:0072136	
GO:2000405	GO:0002627	GO:0016559	GO:0072090	
GO:2000176	GO:0002403	GO:0000266	GO:1903769	
GO:2000175	GO:0002419	GO:0003267	GO:1905474	
GO:2000174	GO:0002424	GO:0003268	GO:1905044	
GO:2000569	GO:0002310	GO:0003269	GO:1905046	
GO:2000568	GO:0002311	GO:0003270	GO:1905045	
GO:2000567	GO:0002361	GO:0003271	GO:1904692	
GO:2000517	GO:0002300	GO:0021937	GO:1904691	
GO:2000525	GO:0002301	GO:0001832	GO:0021921	
GO:2000524	GO:0002303	GO:0001547	GO:0021940	
GO:2000319	GO:0002305	GO:0043029	GO:0021941	
GO:0010820	GO:0002306	GO:0002262	GO:2001013	
GO:0050868	GO:0002307	GO:0033023	GO:1904442	
GO:0050870	GO:0002308	GO:0060248	GO:1904443	
GO:0050856	GO:0002287	GO:0061382	GO:2000795	
GO:0060370	GO:0002288	GO:0036145	GO:2000794	
GO:0036037	GO:0002289	GO:0001782	GO:2000792	
GO:0051141	GO:0002290	GO:0042637	GO:2000791	
GO:0051142	GO:0002293	GO:0021847	GO:2000790	
GO:0051140	GO:0045630	GO:0001550	GO:2000729	
GO:0051138	GO:0045629	GO:0001545	GO:2000607	
GO:0051136	GO:0045627	GO:1990079	GO:2000606	
GO:0051137	GO:0045626	GO:0060250	GO:2000608	
GO:0051134	GO:0033378	GO:0043366	GO:2000137	
GO:0051135	GO:0033379	GO:0007446	GO:2000136	
GO:0051133	GO:0033376	GO:0043930	GO:2000138	
GO:0001916	GO:0033377	GO:0043929	GO:2000566	
GO:0001915	GO:0033380	GO:0002467	GO:2000565	
GO:0001914	GO:0033381	GO:0061519	GO:2000564	
GO:0023022	GO:0033382	GO:0050701	GO:2000563	
GO:0042088	GO:1905398	GO:0001895	GO:2000562	
GO:0072538	GO:1905397	GO:0001894	GO:2000561	
GO:1903904	GO:2001186	GO:0001544	GO:2000497	
GO:1903905	GO:2001187	GO:0001922	GO:2000496	
GO:1900281		GO:0097327	GO:2000495	
GO:1900280		GO:0035986	GO:0060054	
GO:1900279		GO:0046697	GO:0060244	

GO:0045588		GO:0002040	GO:0061006	
GO:0045587		GO:0060249	GO:1904707	
GO:0043378		GO:0061333	GO:1904706	
GO:0043377		GO:0001776	GO:0061331	
GO:0043370		GO:0002119	GO:0061225	
GO:0043372		GO:0061062	GO:0061222	
GO:0043371		GO:0061063	GO:0061269	
GO:0043373		GO:0061064	GO:0090255	
GO:0043376			GO:0090096	
GO:0043375			GO:0090094	
GO:0070237			GO:0014843	
			GO:0072513	
			GO:0061913	
			GO:0061914	
			GO:2000079	
			GO:2000081	

Gene Ontology (GO) Consortium terms for biological processes were used to annotate the genes with mutations in patients and controls.

**Supplementary Table S4. Immune cell subsets in the study patients.**

ID	Disease	EUROClass	TCRg	IgG	IgM	IgA	CD3 (% of lymphocytes)	CD4/CD8 -ratio	NK cells (% of lymphocytes)
1	CVID	B+smB <sup>neg</sup> CD21 <sup>low</sup> Tr <sup>norm</sup>	neg	0.6	<0.10	<0.10	90	0.7	4
2	CVID	B+smB <sup>neg</sup> CD21 <sup>low</sup> Tr <sup>norm</sup>	ND	1.2	1.70	<0.10	86	1.4	10
3	CVID	B-	pos	1.1	0.14	<0.10	90	0.4	9
4	CVID	B+smB+CD21 <sup>norm</sup>	ND	5.50	1.07	0.36	66	2.5	26
5	CVID	B+smB+CD21 <sup>low</sup>	neg	0.60	0.10	0.10	88	1.5	7
6	CVID	B+smB+CD21 <sup>norm</sup>	ND	3.90	0.20	1.24	88	2.3	8
7	CVID	B+smB <sup>neg</sup> CD21 <sup>low</sup> Tr <sup>norm</sup>	ND	1.10	0.27	0.10	85	0.8	6
8	CVID	B-	ND	2.80	0.38	0.00	90	0.6	10
9	<i>STAT3</i> GOF	B+mB <sup>neg</sup> CD21 <sup>low</sup> Tr <sup>norm</sup>	ND	5.6	3.38	1.67	71	1.2	12
10	<i>STAT3</i> GOF	B+mB <sup>neg</sup> CD21 <sup>low</sup> Tr <sup>norm</sup>	pos	2.8	1.44	0.21	86	1.4	3-0.5
11	<i>STAT3</i> GOF	B+smB <sup>neg</sup> CD21 <sup>low</sup> Tr <sup>norm</sup>	ND	0.16	0.6	1.7	74	2.3	4-13
12	Jacobsen sdr	B+smB+CD21 <sup>norm</sup>	pos	3.6	0.81	0.51	87	0.5	9
13	Other	B+smB+CD21 <sup>norm</sup>	neg	2.8	0.92	1.32	70	5.1	23
14	Other	B+smB+CD21 <sup>norm</sup>	neg	8.1	1.01	0.38	72	3.8	12
15	Other	ND	ND	15.1	0.22	0.79	76	4.6	16
16	Good sdr	B-	pos	1.9	<0.10	<0.10	84	0.1	16
17	ADA2 def	B-	pos	0.8	0.24	0.16	99	0.4	<1%

Characteristics of different adaptive immune cells of the patients included in the study are shown. B cell phenotypes were characterized according to the EUROClass classification system.<sup>5</sup>

Abbreviations: ND, not determined; TCRg, T-cell receptor gamma chain rearrangement; pos, positive; neg, negative; sdr, syndrome; GOF, gain-of-function.

**Supplementary Table S5. All somatic mutations identified in paired-sample analyses in CD4+ and CD8+ cells.**

Pt. ID	Disease	Cells	HGVS	AA change	COSMIC	Gene	VAF	SIFT	Poly phen 2
1	CVID	CD8+	1:g.1804503C>G	NM_001282539:exon6:c.G346C:p.G116R		<i>GNB1</i>	0.07	D	D
1	CVID	CD8+	3:g.38580953G>A	NM_198056:exon17:c.C3206T:p.T1069M	COSM1422791,COSM1422790,COSM1422792	<i>SCN5A</i>	0.055	D	D
1	CVID	CD8+	10:g.13136832C>T	NM_001008212:exon15:c.C1700T:p.T567M		<i>OPTN</i>	0.037	D	D
1	CVID	CD8+	19:g.16404674G>A	NM_001258374:exon14:c.C1342T:p.R448C		<i>EPS15L1</i>	0.037	D	D
1	CVID	CD8+	5:g.38881704G>A	NM_001323505:exon4:c.G358A:p.D120N	COSM737822	<i>OSMR</i>	0.035	T	D
2	CVID	CD4+	4:g.105235713delC	NM_001127208:exon3:c.1771delC:p.Q591fs		<i>TET2</i>	0.056	NA	NA
2	CVID	CD4+	4:g.105243618G>T	NM_001127208:exon6:c.G3643T:p.E1215X	COSM3719016	<i>TET2</i>	0.053	NA	NA
2	CVID	CD4+	16:g.50699619G>T	NM_022162:exon2:c.G205T:p.E69X		<i>NOD2</i>	0.06	NA	NA
2	CVID	CD4+	4:g.105269703C>T	NM_001127208:exon9:c.C4138T:p.H1380Y	COSM87161	<i>TET2</i>	0.027	D	D
2	CVID	CD4+	16:g.66398469T>C	NM_001795:exon10:c.T1499C:p.I500T		<i>CDH5</i>	0.027	D	D
2	CVID	CD4+	17:g.42217380A>T	NM_012448:exon10:c.T1254A:p.N418K		<i>STAT5B</i>	0.036	D	D
2	CVID	CD4+	21:g.44426694C>T	NM_001320350:exon27:c.C3980T:p.T1327M	COSM242069	<i>TRPM2</i>	0.036	T	D
2	CVID	CD8+	11:g.89804202C>A	NM_020358:exon3:c.G268T:p.E90X		<i>TRIM49</i>	0.072	NA	NA
2	CVID	CD8+	20:g.62881301C>A	NM_033081:exon16:c.G4655T:p.S1552I		<i>DIDO1</i>	0.086	T	B
3	CVID	CD8+	7:g.100677602C>G	NM_005273:exon6:c.C372G:p.Y124X		<i>GNB2</i>	0.051	NA	NA
3	CVID	CD8+	11:g.75290010T>G	NM_004041:exon2:c.A50C:p.K17T		<i>ARRB1</i>	0.025	D	D
3	CVID	CD8+	17:g.63714087A>C	NM_001003787:exon5:c.T145G:p.S49A		<i>STRADA</i>	0.032	D	D
3	CVID	CD8+	1:g.153337250C>A	NM_020393:exon8:c.G874T:p.V292F		<i>PGLYRP4</i>	0.043	T	D
3	CVID	CD8+	10:g.49646579G>A	NM_020549:exon8:c.G1186A:p.V396M		<i>CHAT</i>	0.024	T	B
4	CVID	CD4+	9:g.5073770G>T	NM_001322195:exon13:c.G1849T:p.V617F	COSM12600	<i>JAK2</i>	0.017	D	D
7	CVID	CD8+	12:g.9090395G>A	NM_000014:exon20:c.C2557T:p.R853W		<i>A2M</i>	0.03	D	D
8	CVID	CD8+	11:g.119028330G>A	NM_001164278:exon4:c.C245T:p.S82F		<i>SLC37A4</i>	0.022	T	B
8	CVID	CD8+	16:g.66617335G>A	NM_178818:exon5:c.C647T:p.T216I		<i>CMTM4</i>	0.021	D	B
12	Jacobsen sdr	CD4+	5:g.83512294C>T	NM_004385:exon6:c.C940T:p.Q314X		<i>VCAN</i>	0.02	NA	NA
12	Jacobsen sdr	CD4+	22:g.36929726C>T	NM_000395:exon6:c.C637T:p.R213W		<i>CSF2RB</i>	0.026	D	D
12	Jacobsen sdr	CD4+	2:g.39336960T>C	NM_003618:exon6:c.A374G:p.Y125C		<i>MAP4K3</i>	0.042	.	D
12	Jacobsen sdr	CD4+	17:g.29098415C>G	NM_078471:exon24:c.G3811C:p.E1271Q		<i>MYO18A</i>	0.027	T	D
12	Jacobsen sdr	CD4+	19:g.47319962C>T	NM_001736:exon2:c.C185T:p.T62M	COSM400357	<i>C5AR1</i>	0.02	T	D
12	Jacobsen sdr	CD8+	2:g.9526225T>A	NM_003183:exon6:c.A639T:p.K213N		<i>ADAM17</i>	0.031	T	P
12	Jacobsen sdr	CD8+	2:g.47839497C>G	NM_001190274:exon3:c.G364C:p.A122P		<i>FBXO11</i>	0.037	T	P
12	Jacobsen sdr	CD8+	X:g.21432736G>A	NM_014927:exon3:c.G353A:p.R118Q		<i>CNKSR2</i>	0.03	T	D
13	Other	CD4+	17:g.42210194G>C	NM_012448:exon15:c.C1883G:p.T628S	COSM6022929	<i>STAT5B</i>	0.032	D	D
15	Other	CD8+	20:g.3706656C>A	NM_023068:exon2:c.G100T:p.G34W		<i>SIGLEC1</i>	0.028	D	D

15	Other	CD8+	22:g.25667739C>G	NM_005160:exon6:c.C442 G:p.P148A		<i>GRK3</i>	0.034	P	P
16	Good sdr	CD4+	3:g.185624078C>T	NM_021627:exon15:c.C16 07T:p.P536L		<i>SENP2</i>	0.035	D	P
16	Good sdr	CD8+	16:g.3243607delT	NM_000243:exon10:c.188 0delA:p.E627fs		<i>MEFV</i>	0.242	NA	NA
16	Good sdr	CD8+	1:g.56692436C>T	NM_006252:exon4:c.C409 T:p.H137Y		<i>PRKAA2</i>	0.032	D	D
16	Good sdr	CD8+	12:g.25227351G>A	NM_004985:exon3:c.C173 T:p.T58I	COSM87288,COSM54905 13	<i>KRAS</i>	0.079	D	D
16	Good sdr	CD8+	15:g.41573360A>T	NM_006293:exon17:c.A20 38T:p.I680F		<i>TYRO3</i>	0.079	D	D
16	Good sdr	CD8+	19:g.13298754G>A	NM_023035:exon19:c.C28 91T:p.A964V		<i>CACNA1A</i>	0.07	T	P
16	Good sdr	CD8+	19:g.19535620G>A	NM_198537:exon6:c.G635 A:p.R212H		<i>YJEFN3</i>	0.292	T	D
16	Good sdr	CD8+	19:g.47320366C>T	NM_001736:exon2:c.C589 T:p.R197W	COSM4667798	<i>C5ARI</i>	0.13	T	P
17	ADA2 def	CD8+	11:g.18026604C>T	NM_004179:exon6:c.G689 A:p.R230H		<i>TPHI</i>	0.029	D	D
17	ADA2 def	CD8+	5:g.138466921G>A	NM_001964:exon2:c.G472 A:p.V158I		<i>EGR1</i>	0.023	D	P
17	ADA2 def	CD8+	12:g.107319038A>G	NM_001018072:exon1:c.A 98G:p.N33S		<i>BTBD11</i>	0.03	T	B
HC1	Healthy	CD8+	9:g.35707732T>C	NM_006289:exon35:c.A46 31G:p.K1544R		<i>TLN1</i>	0.021	T	P
HC3	Healthy	CD8+	15:g.41056702G>A	NM_017553:exon17:c.C19 90T:p.R664C	COSM5383245,COSM538 3244	<i>INO80</i>	0.068	D	D
HC10	Healthy	CD8+	11:g.27674144A>C	NM_001143810:exon2:c.T 141G:p.C47W		<i>BDNF</i>	0.03	D	P
HC10	Healthy	CD8+	19:g.55912295G>C	NLRP13:NM_176810:exo n5:c.C1522G:p.L508V		<i>NLRP13</i>	0.031	T	D
HC11	Healthy	CD8+	2:g.25240306A>G	NM_175629:exon19:c.T23 18C:p.L773P	COSM1583115	<i>DNMT3A</i>	0.043	D	D
HC11	Healthy	CD8+	5:g.170270842C>G	NM_005565:exon7:c.G400 C:p.E134Q		<i>LCP2</i>	0.045	T	P
HC11	Healthy	CD8+	9:g.130880097T>C	NM_007313:exon9:c.T151 0C:p.S504P		<i>ABL1</i>	0.059	D	P
HC15	Healthy	CD8+	3:g.49302514A>G	NM_003363:exon10:c.T11 57C:p.F386S		<i>USP4</i>	0.043	D	D
HC15	Healthy	CD8+	5:g.111072933G>A	NM_033035:exon2:c.216+ 1G>A		<i>TSLP</i>	0.049	NA	NA
HC16	Healthy	CD8+	3:g.184365148T>G	NM_001278698:exon3:c.T 173G:p.L58W		<i>POLR2H</i>	0.032	D	D
HC16	Healthy	CD8+	4:g.38797118T>C	NM_003263:exon4:c.A171 4G:p.M572V		<i>TLR1</i>	0.021	T	B
HC16	Healthy	CD8+	19:g.51501460G>A	NM_053003:exon1:c.C274 T:p.R92X	COSM4766319	<i>SIGLEC12</i>	0.023	NA	NA
HC17	Healthy	CD4+	7:g.2002123T>A	NM_001013836:exon15:c. 1360-2A>T		<i>MADIL1</i>	0.044	NA	NA
HC17	Healthy	CD4+	19:g.51458037C>G	NM_014442:exon1:c.G351 C:p.R117S		<i>SIGLEC8</i>	0.024	T	B
HC17	Healthy	CD8+	5:g.148827319T>G	NM_000024:exon1:c.T488 G:p.L163R		<i>ADRB2</i>	0.057	D	D
HC17	Healthy	CD8+	15:g.74036026C>G	NM_033247:exon5:c.C127 4G:p.A425G		<i>PML</i>	0.025	T	B
HC17	Healthy	CD8+	16:g.31266064A>T	NM_001145808:exon5:c.A 344T:p.E115V		<i>ITGAM</i>	0.05	D	P
HC17	Healthy	CD8+	21:g.31251838C>G	NM_003253:exon6:c.G131 5C:p.A439P		<i>TIAM1</i>	0.029	T	D
HC17	Healthy	CD8+	21:g.31266560T>A	NM_003253:exon5:c.A413 T:p.D138V		<i>TIAM1</i>	0.047	D	P
HC18	Healthy	CD8+	7:g.84011182C>T	NM_006080:exon9:c.925+ 1G>A		<i>SEMA3A</i>	0.037	NA	NA
HC18	Healthy	CD8+	8:g.99192975A>G	NM_017890:exon17:c.A24 33G:p.I811M		<i>VPS13B</i>	0.02	D	P
HC18	Healthy	CD8+	12:g.7499159G>A	NM_004244:exon4:c.C487 T:p.R163C	COSM4670363,COSM467 0362	<i>CD163</i>	0.034	D	B
HC18	Healthy	CD8+	14:g.68880046C>G	NM_001130004:exon18:c. G2196C:p.E732D		<i>ACTN1</i>	0.02	T	P
HC18	Healthy	CD8+	18:g.23556356T>C	NM_000271:exon8:c.A121 3G:p.T405A		<i>NPC1</i>	0.028	T	B
HC20	Healthy	CD8+	7:g.48508005C>A	NM_152701:exon50:c.C13 480A:p.L4494I		<i>ABCA13</i>	0.029	T	D



HC20	Healthy	CD8+	10:g.122576623C>T	NM_001320644:exon7:c.C508T:p.R170C	COSM3367939,COSM3367940,COSM3367938	<i>DMBT1</i>	0.042	T	D
HC20	Healthy	CD8+	11:g.129870009T>C	NM_006165:exon22:c.A3091G:p.I1031V		<i>NFRKB</i>	0.054	T	P
HC21	Healthy	CD4+	1:g.114716123C>T	NM_002524:exon2:c.G38A:p.G13D	COSM573	<i>NRAS</i>	0.018	D	B

All mutations discovered in healthy controls and immunodeficiency patients in CD4+ and CD8+ cells by paired-sample analyses by MuTect2. Abbreviations: Pt., patient; AA, amino acid; VAF, variant allele frequency; SIFT, SIFT prediction; PolyPhen2, Polyphen2 HDIV prediction; T, tolerated; D, deleterious (SIFT)/probably damaging (PolyPhen2); B, benign; P, possibly damaging; NA, not available (splice-site, frameshift, or nonsense variant).

**Supplementary table S6. Somatic mutations in T cells do not occur in non-hematopoietic tissue samples.**

Pt. ID	Disease	HGVS	AA change	Gene	VAF in CD8+	CD8+		CD4+		Skin	
						Variant reads	Normal reads	Variant reads	Normal reads	Variant reads	Normal reads
7	CVID	12:g.9090395G>A	NM_000014:exon20:c.C2557T:p.R853W	<i>A2M</i>	0.03	14	462	0	535	0	427
15	Other	20:g.3706656C>A	NM_023068:exon2:c.G100T:p.G34W	<i>SIGLEC1</i>	0.028	11	331	0	285	0	359
15	Other	22:g.25667739C>G	NM_005160:exon6:c.C442G:p.P148A	<i>GRK3</i>	0.034	25	692	0	740	0	765

Most of our data on somatic mutations has been called using paired-sample comparisons between CD4+ and CD8+ cells. However, from two patients, we had DNA available from non-hematopoietic tissues (patient 7: skin fibroblasts; patient 15: skin biopsy). These samples were sequenced with the same sequencing panel as CD4+ and CD8+ cells. The table shows the sequencing results from these patient samples. Somatic variants were called using a paired-sample strategy, CD4+ cells vs. CD8+ and *vice versa*, but also using the non-hematopoietic tissue sample as a control sample. Three different somatic variants were identified in these patients, but the variants were discovered to exist only in CD8+ cells, regardless of which germline control (CD4+ or non-hematopoietic tissue) was used. Only CD8+ cells harbored sequencing reads that supported the variant; these reads did not exist in CD4+ or in non-hematopoietic tissue samples. Abbreviations: Pt., patient; AA, amino acid; VAF, variant allele frequency.

**Supplementary Table S7. Mapped bases in sequenced samples.**

ID	Disease	Sex	Age	Mapped bases CD4+	Mapped bases CD8+	Library
1	CVID	M	61	5 547 239 430	5 264 291 170	Kapa
2	CVID	M	67	5 605 211 973	4 424 304 170	Kapa
3	CVID	M	54	6 425 897 948	6 289 169 731	Kapa
4	CVID	M	70	7 913 485 919	8 249 467 672	Kapa
5	CVID	F	70	6 111 957 589	5 949 483 474	Kapa
6	CVID	F	67	8 409 971 358	7 793 689 636	Kapa
7	CVID	F	35	5 794 543 945	5 843 367 134	Kapa
8	CVID	M	37	5 843 723 928	5 172 024 026	Kapa
9	STAT3 GOF	F	17	5 893 167 691	5 986 103 640	Kapa
10	STAT3 GOF	F	15	6 686 032 805	6 307 531 709	Kapa
11	STAT3 GOF	F	22	6 283 989 638	5 740 280 375	Kapa
12	Jacobsen sdr	F	46	9 142 391 648	9 203 546 364	Kapa
13	Other	F	73	8 908 263 746	8 932 451 607	Kapa
14	Other	F	70	6 227 668 622	6 191 344 170	Kapa
15	Other	M	60	5 880 893 385	6 520 578 161	Kapa
16	Good sdr	M	70	5 799 566 210	6 230 264 907	Kapa
17	ADA2 deficiency	F	41	5 944 877 329	6 040 071 375	Kapa
HC1	HC	F	58	4 836 247 489	4 907 094 913	Kapa
HC10	HC	F	47	3 332 774 616	3 000 407 005	ThruPLEX
HC11	HC	M	48	3 006 395 425	3 839 564 953	ThruPLEX
HC12	HC	F	21	1 537 950 784	3 041 728 643	ThruPLEX
HC13	HC	F	66	5 178 847 798	4 906 517 851	Kapa
HC14	HC	F	63	3 915 254 480	4 303 882 913	Kapa
HC15	HC	M	63	4 255 679 405	4 062 759 031	Kapa
HC16	HC	F	65	5 326 558 097	5 534 346 901	Kapa
HC17	HC	M	64	5 485 499 484	5 668 209 736	Kapa
HC18	HC	F	65	4 360 042 314	4 283 227 672	Kapa
HC19	HC	M	64	4 324 897 537	4 645 201 325	Kapa
HC2	HC	M	58	4 840 430 099	4 898 833 343	Kapa
HC20	HC	F	63	4 651 864 808	4 815 541 862	Kapa
HC21	HC	M	64	4 688 775 892	4 567 660 361	Kapa
HC3	HC	F	65	5 001 034 164	5 223 776 490	Kapa
HC4	HC	F	44	3 377 389 646	2 296 486 796	ThruPLEX
HC5	HC	M	55	2 865 922 283	3 585 929 964	ThruPLEX
HC6	HC	M	52	3 163 636 155	4 482 310 699	ThruPLEX
HC7	HC	M	48	1 332 951 785	3 315 440 185	ThruPLEX
HC8	HC	F	57	3 012 854 365	3 367 018 062	ThruPLEX
HC9	HC	F	56	3 083 658 397	2 669 438 976	ThruPLEX

The numbers of mapped bases in immunogene sequencing for healthy controls and immunodeficiency patients. Abbreviations: HC, healthy control; GOF, gain-of-function; sdr,

syndrome; Library, sequencing library preparation kit; Kapa, Kapa Hyper library preparation kit (Roche); ThruPLEX, ThruPLEX DNA-seq Library Preparation Kit (Rubicon Genomics).

**Supplementary Table S8. Clonal hematopoiesis variants occurring in both CD4+ and CD8+ cells.**

Patient	AA change	Consequence	CD4+ (VAF)	CD8+ (VAF)	Targeted deep seq of sorted cells (VAF)				
					CD3+ CD4+	CD3+ CD8+	CD19+	CD14+	WB
13	<i>DNMT3A</i> :NM_022552:exon 20:c.2388dupT;p.N797_L798delinsX	nonsense	0.043	0.038	0.046	0.030	0.027	0	0.037
2	<i>TET2</i> :NM_001127208:exon 6:c.G3643T;p.E1215X	nonsense	0.053	0.027	0.039	0	0.040	0	0.010
2	<i>TET2</i> :NM_001127208:exon 11:c.C4889G;p.S1630X	nonsense	0.041	0.032	0.037	0.023	0	0	0

We performed a sorting and sequencing experiment to investigate in which cell types the variants associated with clonal hematopoiesis existed. CD3+CD4+, CD3+CD8+, CD19+, CD14+ and whole-blood cells were sequenced with targeted deep Amplicon sequencing. The VAFs in each cell fraction are shown in the table. In addition to T-cell fractions, mutations were also found in CD19+ B cells, but not in CD14+ monocytes. Abbreviations: VAF, variant allele frequency; AA, amino acid; WB, whole blood.

**Supplementary Table S9. The sequencing panel for mutation validations.**

Gene name	Control position or somatic variant?	Chr	Position (GRCh38)	COSMIC identifier
<i>GNB1</i>	control	1	1815790	COSM211450
<i>TET2</i>	control	4	105276128	COSM41741
<i>NOD2</i>	control	16	50710787	COSM2834328
<i>GNB2</i>	control	7	100678546	COSM4687440
<i>JAK2</i>	control	9	5078360	COSM29300
<i>A2M</i>	control	12	9112203	COSM1177109
<i>CSF2RB</i>	control	22	36936577	COSM4411434
<i>STAT5B</i>	control	17	42202370	COSM1716827
<i>SIGLEC1</i>	control	20	3694821	COSM84704
<i>KRAS</i>	control	12	25245350	COSM521
<i>C5ARI</i>	control	19	47320786	COSM1751014
<i>EGR1</i>	control	5	138467408	COSM74487
<i>DNMT3A</i>	control	2	25234373	COSM52944
<i>SIGLEC12</i>	control	19	51499608	COSM116869
<i>CD163</i>	control	12	7486950	COSM298612
<i>DMBT1</i>	control	10	122643283	COSM1346480
<i>NRAS</i>	control	1	114713909	COSM580
<i>GNB1</i>	somatic variant	1	1804503	
<i>TET2</i>	somatic variant	4	105235713	
<i>TET2</i>	somatic variant	4	105243618	COSM3719016
<i>NOD2</i>	somatic variant	16	50699619	
<i>TET2</i>	somatic variant	4	105269703	COSM87161
<i>STAT5B</i>	somatic variant	17	42217380	
<i>GNB2</i>	somatic variant	7	100677602	
<i>JAK2</i>	somatic variant	9	5073770	COSM12600
<i>A2M</i>	somatic variant	12	9090395	
<i>CSF2RB</i>	somatic variant	22	36929726	
<i>STAT5B</i>	somatic variant	17	42210194	COSM6022929
<i>SIGLEC1</i>	somatic variant	20	3706656	
<i>KRAS</i>	somatic variant	12	25227351	COSM87288,COSM5490513
<i>C5ARI</i>	somatic variant	19	47320366	COSM4667798
<i>EGR1</i>	somatic variant	5	138466921	
<i>DNMT3A</i>	somatic variant	2	25240306	COSM1583115
<i>SIGLEC12</i>	somatic variant	19	51501460	COSM4766319
<i>CD163</i>	somatic variant	12	7499159	COSM4670363,COSM4670362
<i>DMBT1</i>	somatic variant	10	122576623	COSM3367939,COSM3367940,COSM3367938
<i>NRAS</i>	somatic variant	1	114716123	COSM573
<i>DNMT3A</i>	somatic variant	2	25239149	
<i>TET2</i>	somatic variant	4	105235712	

---

<i>TET2</i>	somatic variant	4	105275399	COSM5945066
<i>DNMT3A</i>	somatic variant	2	25244616	COSM1583077

---

A ParagonGenomics CleanPlex Custom Amplicon panel was designed to perform confirmative a sequencing experiment on the discovered somatic mutations. Positions covered by the multiplex panel are listed above. The panel included 24 mutation positions and 17 control positions. The individual with the *SIGLEC12* mutation (HC16) was not included in sequencing due to sample amount restraints, although the position was included in the panel.

**Supplementary Table S10. Confirmatory Amplicon sequencing on selected variants.**

Pt. ID	Disease	Cells	HGVS	AA change	Gene	VAF in immunopanel	VAF in amplicon sequencing
1	CVID	CD8+	1:g.1804503C>G	NM_001282539:exon6:c.G346C:p.G116R	<i>GNB1</i>	0.07	0.056
2	CVID	CD4+	17:g.42217380A>T	NM_012448:exon10:c.T1254A:p.N418K	<i>STAT5B</i>	0.036	0.060
2	CVID	CD4+	4:g.105243618G>T	NM_001127208:exon6:c.G3643T:p.E1215X	<i>TET2</i>	0.053	0.026
2	CVID	CD4+	16:g.50699619G>T	NM_022162:exon2:c.G205T:p.E69X	<i>NOD2</i>	0.06	0.064
2	CVID	CD4+	4:g.105269703C>T	NM_001127208:exon9:c.C4138T:p.H1380Y	<i>TET2</i>	0.027	0.020
3	CVID	CD8+	7:g.100677602C>G	NM_005273:exon6:c.C372G:p.Y124X	<i>GNB2</i>	0.051	0.038
7	CVID	CD8+	12:g.9090395G>A	NM_000014:exon20:c.C2557T:p.R853W	<i>A2M</i>	0.03	0.029
12	Jacobsen sdr	CD4+	22:g.36929726C>T	NM_000395:exon6:c.C637T:p.R213W	<i>CSF2RB</i>	0.026	0.015
13	Other	CD4+	17:g.42210194G>C	NM_012448:exon15:c.C1883G:p.T628S	<i>STAT5B</i>	0.032	0.035
15	Other	CD8+	20:g.3706656C>A	NM_023068:exon2:c.G100T:p.G34W	<i>SIGLEC1</i>	0.028	0.023
16	Good sdr	CD8+	12:g.25227351G>A	NM_004985:exon3:c.C173T:p.T58I	<i>KRAS</i>	0.079	0.073
16	Good sdr	CD8+	19:g.47320366C>T	NM_001736:exon2:c.C589T:p.R197W	<i>C5ARI</i>	0.13	0.101
17	ADA2 def	CD8+	5:g.138466921G>A	NM_001964:exon2:c.G472A:p.V158I	<i>EGR1</i>	0.023	0.031
HC11	Healthy	CD8+	2:g.25240306A>G	NM_175629:exon19:c.T2318C:p.L773P	<i>DNMT3A</i>	0.043	0.034
HC18	Healthy	CD8+	12:g.7499159G>A	NM_004244:exon4:c.C487T:p.R163C	<i>CD163</i>	0.034	0.031
HC20	Healthy	CD8+	10:g.122576623C>T	NM_001320644:exon7:c.C508T:p.R170C	<i>DMBT1</i>	0.042	0.036
HC21	Healthy	CD4+	1:g.114716123C>T	NM_002524:exon2:c.G38A:p.G13D	<i>NRAS</i>	0.018	0.023

Amplicon sequencing was performed to confirm a subset of somatic mutations. The table shows the mutations identified by paired-sample calling in immunogene panel sequencing. Mutations associated with clonal hematopoiesis are presented in Supplementary Table S8. The variant allele frequencies (VAFs), determined by both immunogene panel and amplicon sequencing, are shown. Abbreviations: Pt., patient; AA, amino acid; VAF, variant allele frequency. All variants that were covered by sufficient sequencing depth were confirmed by an independent method, targeted deep amplicon sequencing.



**Supplementary Table S11. Amino-acid properties of convergent and highly expanded TCRs.**

		Peptide hydrophobicity	Charge	PP1 (~polarity)	PP2 (~hydrophobicity)	PP3 (~Hydrogen bonding)
CD8+ highly convergent	Difference between means	-0.0988	0.0329	0.0297	0.0073	-0.0064
	CI lower	-0.1339	-0.0352	0.0190	0.0015	-0.0133
	CI higher	-0.0637	0.1011	0.0405	0.0131	0.0006
	p-value	<b>3.696*10E-08</b>	0.3429	<b>6.321*10E-08</b>	<b>0.0137</b>	0.0731
CD8+ Highly expanded	Difference between means	-0.0681	-0.1623	0.0220	0.0030	-0.0201
	CI lower	-0.2150	-0.4666	-0.0254	-0.0219	-0.0520
	CI higher	0.0788	0.1420	0.0694	0.0278	0.0118
	p-value	0.3607	0.2934	0.3593	0.8131	0.2136
CD4+ Highly convergent	Difference between means	-0.0196	0.0306	-0.0005	-0.0021	0.0120
	CI lower	-0.1192	-0.1467	-0.0289	-0.0188	-0.0055
	CI higher	0.0801	0.2078	0.0279	0.0146	0.0295
	p-value	0.6993	0.7342	0.9703	0.8042	0.1789
CD4+ Highly expanded	Difference between means	0.0639	0.0765	-0.0101	-0.0045	0.0166
	CI lower	-0.0739	-0.1597	-0.0488	-0.0264	-0.0069
	CI higher	0.2017	0.3127	0.0287	0.0173	0.0402
	p-value	0.3613	0.5233	0.6083	0.6810	0.1652

The amino-acid properties (PP1, PP2, and PP3 by Cruciani *et al*)<sup>14</sup> were compared between selected TCR subsets between CVID patients and healthy controls by a Welch T-test. No multiple comparison adjustments were made. The table shows the test p-values, differences between means (CVID vs healthy), and 95% confidence intervals for the difference between means. “Highly convergent” and “highly expanded” TCR definitions are included in the Methods-section. CVID CD8+ convergent TCRs showed differential physico-chemical properties when compared to healthy controls’ convergent TCRs, but no differences existed between CVID and controls in CD4+ cells, or “highly expanded” CD8+ TCRs. Abbreviations: HC, healthy control.

**Supplementary Table S12. T-cell clone sizes and mutation VAFs.**

Pt. ID	Disease	Cells	Gene	AA change	HGVS	max clone size	VAF
1	CVID	CD8+	<i>GNB1</i>	NM_001282539:exon6:c.G346C:p.G116R	1:g.1804503C>G	0.173069224	0.07
1	CVID	CD8+	<i>SCN5A</i>	NM_198056:exon17:c.C3206T:p.T1069M	3:g.38580953G>A	0.173069224	0.055
1	CVID	CD8+	<i>OPTN</i>	NM_001008212:exon15:c.C1700T:p.T567M	10:g.13136832C>T	0.173069224	0.037
1	CVID	CD8+	<i>EPS15L1</i>	NM_001258374:exon14:c.C1342T:p.R448C	19:g.16404674G>A	0.173069224	0.037
1	CVID	CD8+	<i>OSMR</i>	NM_001323505:exon4:c.G358A:p.D120N	5:g.38881704G>A	0.173069224	0.035
2	CVID	CD4+	<i>TET2</i>	NM_001127208:exon3:c.1771delC:p.Q591fs	4:g.105235713delC	0.004372718829553281	0.056
2	CVID	CD4+	<i>TET2</i>	NM_001127208:exon6:c.G3643T:p.E1215X	4:g.105243618G>T	0.004372718829553281	0.053
2	CVID	CD4+	<i>NOD2</i>	NM_022162:exon2:c.G205T:p.E69X	16:g.50699619G>T	0.004372718829553281	0.06
2	CVID	CD4+	<i>TET2</i>	NM_001127208:exon9:c.C4138T:p.H1380Y	4:g.105269703C>T	0.004372718829553281	0.027
2	CVID	CD4+	<i>CDH5</i>	NM_001795:exon10:c.T1499C:p.I500T	16:g.66398469T>C	0.004372718829553281	0.027
2	CVID	CD4+	<i>STAT5B</i>	NM_012448:exon10:c.T1254A:p.N418K	17:g.42217380A>T	0.004372718829553281	0.036
2	CVID	CD4+	<i>TRPM2</i>	NM_001320350:exon27:c.C3980T:p.T1327M	21:g.44426694C>T	0.004372718829553281	0.036
2	CVID	CD8+	<i>TRIM49</i>	NM_020358:exon3:c.G268T:p.E90X	11:g.89804202C>A	0.202465609	0.072
2	CVID	CD8+	<i>DIDO1</i>	NM_033081:exon16:c.G4655T:p.S1552I	20:g.62881301C>A	0.202465609	0.086
3	CVID	CD8+	<i>GNB2</i>	NM_005273:exon6:c.C372G:p.Y124X	7:g.100677602C>G	0.0646392182	0.051
3	CVID	CD8+	<i>ARRB1</i>	NM_004041:exon2:c.A50C:p.K17T	11:g.75290010T>G	0.0646392182	0.025
3	CVID	CD8+	<i>STRADA</i>	NM_001003787:exon5:c.T145G:p.S49A	17:g.63714087A>C	0.0646392182	0.032
3	CVID	CD8+	<i>PGLYRP4</i>	NM_020393:exon8:c.G874T:p.V292F	1:g.153337250C>A	0.0646392182	0.043
3	CVID	CD8+	<i>CHAT</i>	NM_020549:exon8:c.G1186A:p.V396M	10:g.49646579G>A	0.0646392182	0.024
4	CVID	CD4+	<i>JAK2</i>	NM_001322195:exon13:c.G1849T:p.V617F	9:g.5073770G>T	0.002205217535162855	0.017
7	CVID	CD8+	<i>A2M</i>	NM_000014:exon20:c.C2557T:p.R853W	12:g.9090395G>A	0.0647578761	0.03
8	CVID	CD8+	<i>SLC37A4</i>	NM_001164278:exon4:c.C245T:p.S82F	11:g.119028330G>A	NA	0.022
8	CVID	CD8+	<i>CMTM4</i>	NM_178818:exon5:c.C647T:p.T216I	16:g.66617335G>A	NA	0.021
12	Jacobsen syndrome	CD4+	<i>VCAN</i>	NM_004385:exon6:c.C940T:p.Q314X	5:g.83512294C>T	0.0717540607	0.02
12	Jacobsen syndrome	CD4+	<i>CSF2RB</i>	NM_000395:exon6:c.C637T:p.R213W	22:g.36929726C>T	0.0717540607	0.026
12	Jacobsen syndrome	CD4+	<i>MAP4K3</i>	NM_003618:exon6:c.A374G:p.Y125C	2:g.39336960T>C	0.0717540607	0.042
12	Jacobsen syndrome	CD4+	<i>MYO18A</i>	NM_078471:exon24:c.G3811C:p.E1271Q	17:g.29098415C>G	0.0717540607	0.027
12	Jacobsen syndrome	CD4+	<i>C5AR1</i>	NM_001736:exon2:c.C185T:p.T62M	19:g.47319962C>T	0.0717540607	0.02
12	Jacobsen syndrome	CD8+	<i>ADAM17</i>	NM_003183:exon6:c.A639T:p.K213N	2:g.9526225T>A	0.110719606	0.031
12	Jacobsen syndrome	CD8+	<i>FBXO11</i>	NM_001190274:exon3:c.G364C:p.A122P	2:g.47839497C>G	0.110719606	0.037
12	Jacobsen syndrome	CD8+	<i>CNKSR2</i>	NM_014927:exon3:c.G353A:p.R118Q	X:g.21432736G>A	0.110719606	0.03
13	Other	CD4+	<i>STAT5B</i>	NM_012448:exon15:c.C1883G:p.T628S	17:g.42210194G>C	8.97995840678191E-4	0.032
15	Other	CD8+	<i>SIGLEC1</i>	NM_023068:exon2:c.G100T:p.G34W	20:g.3706656C>A	0.0996980518	0.028
15	Other	CD8+	<i>GRK3</i>	NM_005160:exon6:c.C442G:p.P148A	22:g.25667739C>G	0.0996980518	0.034
16	Good syndrome	CD4+	<i>SENP2</i>	NM_021627:exon15:c.C1607T:p.P536L	3:g.185624078C>T	0.0307179019	0.035
16	Good syndrome	CD8+	<i>MEFV</i>	NM_000243:exon10:c.1880delA:p.E627fs	16:g.3243607delT	0.512191474	0.242
16	Good syndrome	CD8+	<i>PRKAA2</i>	NM_006252:exon4:c.C409T:p.H137Y	1:g.56692436C>T	0.512191474	0.032
16	Good syndrome	CD8+	<i>KRAS</i>	NM_004985:exon3:c.C173T:p.T58I	12:g.25227351G>A	0.512191474	0.079
16	Good syndrome	CD8+	<i>TYRO3</i>	NM_006293:exon17:c.A2038T:p.I680F	15:g.41573360A>T	0.512191474	0.079
16	Good syndrome	CD8+	<i>CACNA1A</i>	NM_023035:exon19:c.C2891T:p.A964V	19:g.13298754G>A	0.512191474	0.07
16	Good syndrome	CD8+	<i>YJEFN3</i>	NM_198537:exon6:c.G635A:p.R212H	19:g.19535620G>A	0.512191474	0.292

16	Good syndrome	CD8+	<i>C5AR1</i>	NM_001736:exon2:c.C589T:p.R197W	19:g.47320366C>T	0.512191474	0.13
17	ADA2 deficiency	CD8+	<i>TPH1</i>	NM_004179:exon6:c.G689A:p.R230H	11:g.18026604C>T	NA	0.029
17	ADA2 deficiency	CD8+	<i>EGR1</i>	NM_001964:exon2:c.G472A:p.V158I	5:g.138466921G>A	NA	0.023
17	ADA2 deficiency	CD8+	<i>BTBD11</i>	NM_001018072:exon1:c.A98G:p.N33S	12:g.107319038A>G	NA	0.03
HC1	Healthy	CD8+	<i>TLN1</i>	NM_006289:exon35:c.A4631G:p.K1544R	9:g.35707732T>C	0.118211403	0.021
HC3	Healthy	CD8+	<i>INO80</i>	NM_017553:exon17:c.C1990T:p.R664C	15:g.41056702G>A	0.24665913	0.068
HC10	Healthy	CD8+	<i>BDNF</i>	NM_001143810:exon2:c.T141G:p.C47W	11:g.27674144A>C	0.0707740486	0.03
HC10	Healthy	CD8+	<i>NLRP13</i>	NLRP13:NM_176810:exon5:c.C1522G:p.L508V	19:g.55912295G>C	0.0707740486	0.031
HC11	Healthy	CD8+	<i>DNMT3A</i>	NM_175629:exon19:c.T2318C:p.L773P	2:g.25240306A>G	0.110654257	0.043
HC11	Healthy	CD8+	<i>LCP2</i>	NM_005565:exon7:c.G400C:p.E134Q	5:g.170270842C>G	0.110654257	0.045
HC11	Healthy	CD8+	<i>ABL1</i>	NM_007313:exon9:c.T1510C:p.S504P	9:g.130880097T>C	0.110654257	0.059
HC15	Healthy	CD8+	<i>USP4</i>	NM_003363:exon10:c.T1157C:p.F386S	3:g.49302514A>G	0.065790467	0.043
HC15	Healthy	CD8+	<i>TSLP</i>	NM_033035:exon2:c.216+1G>A	5:g.111072933G>A	0.065790467	0.049
HC16	Healthy	CD8+	<i>POLR2H</i>	NM_001278698:exon3:c.T173G:p.L58W	3:g.184365148T>G	0.114472464	0.032
HC16	Healthy	CD8+	<i>TLR1</i>	NM_003263:exon4:c.A1714G:p.M572V	4:g.38797118T>C	0.114472464	0.021
HC16	Healthy	CD8+	<i>SIGLEC12</i>	NM_053003:exon1:c.C274T:p.R92X	19:g.51501460G>A	0.114472464	0.023
HC17	Healthy	CD4+	<i>MAD1L1</i>	NM_001013836:exon15:c.1360-2A>T	7:g.2002123T>A	0.185848787	0.044
HC17	Healthy	CD4+	<i>SIGLEC8</i>	NM_014442:exon1:c.G351C:p.R117S	19:g.51458037C>G	0.185848787	0.024
HC17	Healthy	CD8+	<i>ADRB2</i>	NM_000024:exon1:c.T488G:p.L163R	5:g.148827319T>G	0.0644821748	0.057
HC17	Healthy	CD8+	<i>PML</i>	NM_033247:exon5:c.C1274G:p.A425G	15:g.74036026C>G	0.0644821748	0.025
HC17	Healthy	CD8+	<i>ITGAM</i>	NM_001145808:exon5:c.A344T:p.E115V	16:g.31266064A>T	0.0644821748	0.05
HC17	Healthy	CD8+	<i>TIAMI</i>	NM_003253:exon6:c.G1315C:p.A439P	21:g.31251838C>G	0.0644821748	0.029
HC17	Healthy	CD8+	<i>TIAMI</i>	NM_003253:exon5:c.A413T:p.D138V	21:g.31266560T>A	0.0644821748	0.047
HC18	Healthy	CD8+	<i>SEMA3A</i>	NM_006080:exon9:c.925+1G>A	7:g.84011182C>T	0.136208773	0.037
HC18	Healthy	CD8+	<i>VPS13B</i>	NM_017890:exon17:c.A2433G:p.I811M	8:g.99192975A>G	0.136208773	0.02
HC18	Healthy	CD8+	<i>CD163</i>	NM_004244:exon4:c.C487T:p.R163C	12:g.7499159G>A	0.136208773	0.034
HC18	Healthy	CD8+	<i>ACTN1</i>	NM_001130004:exon18:c.G2196C:p.E732D	14:g.68880046C>G	0.136208773	0.02
HC18	Healthy	CD8+	<i>NPC1</i>	NM_000271:exon8:c.A1213G:p.T405A	18:g.23556356T>C	0.136208773	0.028
HC20	Healthy	CD8+	<i>ABCA13</i>	NM_152701:exon50:c.C13480A:p.L4494I	7:g.48508005C>A	0.0919760615	0.029
HC20	Healthy	CD8+	<i>DMBT1</i>	NM_001320644:exon7:c.C508T:p.R170C	10:g.122576623C>T	0.0919760615	0.042
HC20	Healthy	CD8+	<i>NFRKB</i>	NM_006165:exon22:c.A3091G:p.I1031V	11:g.129870009T>C	0.0919760615	0.054
HC21	Healthy	CD4+	<i>NRAS</i>	NM_002524:exon2:c.G38A:p.G13D	1:g.114716123C>T	8.011564664076844E-4	0.018

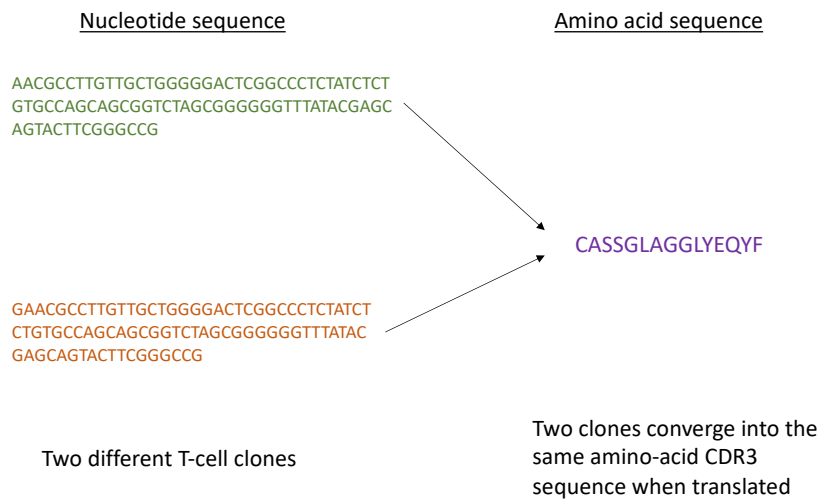
The table shows each mutation discovered in the paired-sample mutation analyses. The cell type harboring the mutation is shown (CD4+ or CD8+). Also, the “max clone size” -column shows the frequency of the largest T-cell clone of all of the sequenced cells (CD4+ or CD8+). The clone frequency shown always corresponds to the cell fraction in which the mutation was discovered.

**Supplementary Table S13. *STAT5B* and *KRAS* mutations in sorted T cells.**

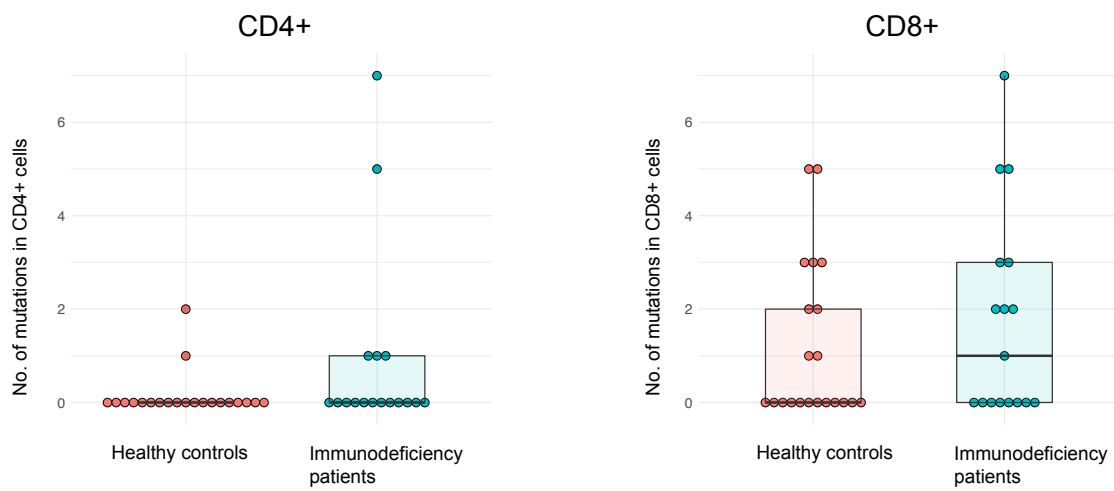
Patient	Gene	AA change	Variant allele frequency			
			CD3+CD4+	CD3+CD8+	CD14+	CD3 <sup>neg</sup> CD14 <sup>neg</sup>
Pt.2	<i>STAT5B</i>	N418K	0.069	0*	0	0
Pt.13	<i>STAT5B</i>	T628S	0.048	0	0	0
Pt.26	<i>KRAS</i>	T58I	0	0.075	0	Not sorted

Flow-cytometry-mediated sorting was used to extract CD3+ T cells and other cell types for sequencing. The *STAT5B* mutations occurred only in CD3+CD4+ cells, and the *KRAS* only in CD3+CD8+ cells. \*For patient 2, CD3+CD8+ T cells were sorted also according to the largest CD3+CD8+Vbeta expansion, but both Vbeta+ and Vbeta<sup>neg</sup> fractions were negative. Abbreviations: AA, amino acid.

## Supplementary Figure S1. T-cell clones and convergence of clones.

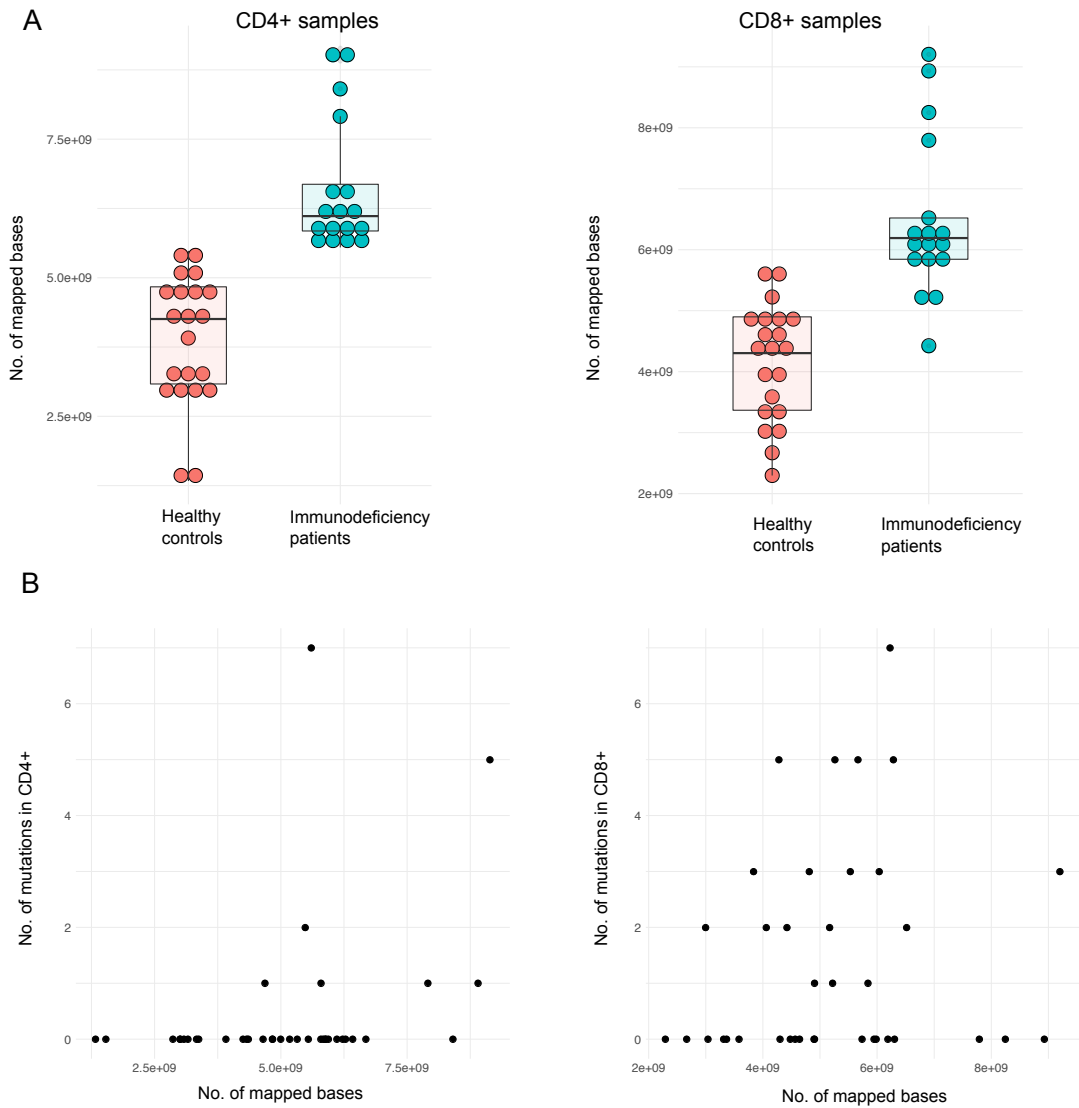


**Supplementary Figure S2. The number of discovered mutations in patients and controls.**



The number of somatic mutations in CD4+ or CD8+ cells did not differ between immunodeficiency patients and controls (Mann-Whitney test). The plots show the number of mutations in each studied individual, with vertical lines representing the median, box hinges interquartile ranges, and whiskers reasonable extremes of the data.

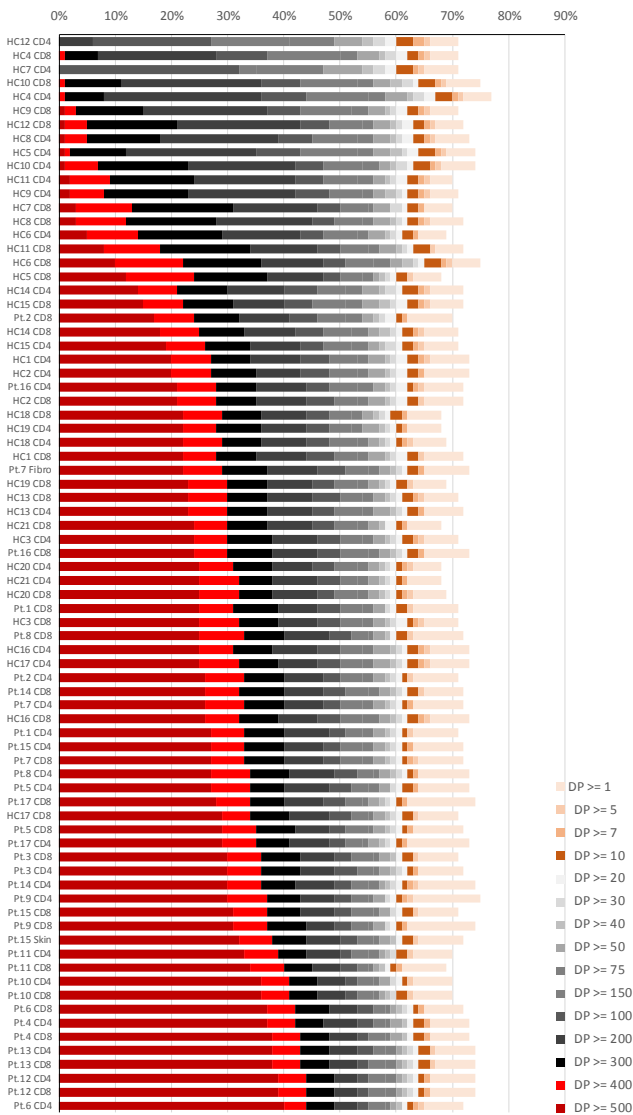
**Supplementary Figure S3. The numbers of mapped bases in CD4+ and CD8+ cells.**



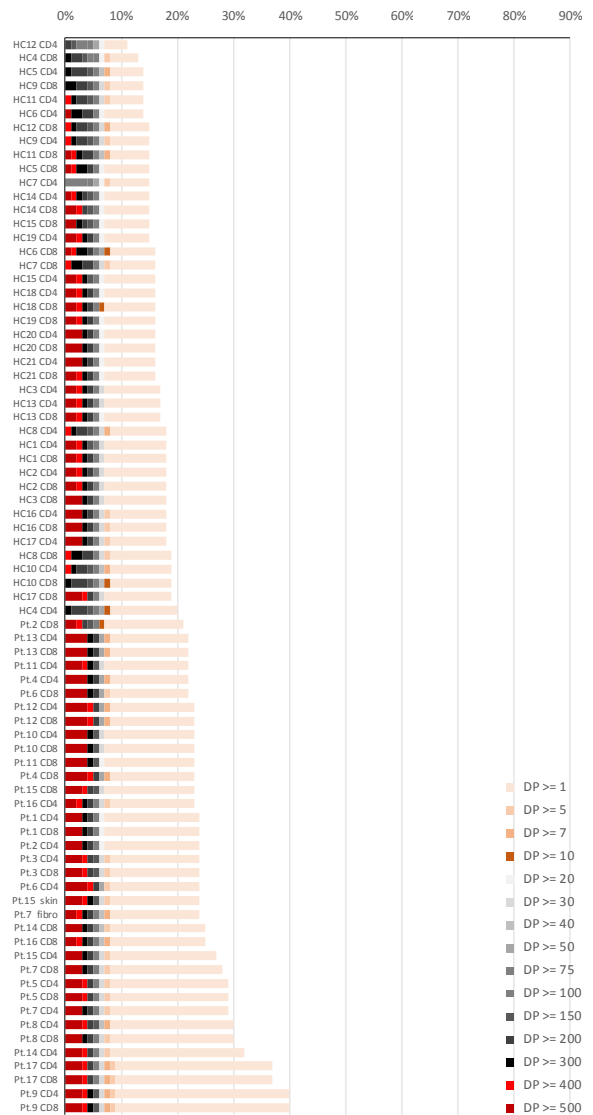
The numbers of mapped bases in immunogene sequencing for healthy controls and immunodeficiency patients. Results for CD4+ and CD8+ samples are shown separately. A. Immunodeficiency patients had higher numbers of mapped bases in CD8+ samples (p-value = 4.753e-08, Mann-Whitney test) and in CD4+ samples (p-value = 6.949e-11, Mann-Whitney test). Boxplot hinges represent interquartile medians and the vertical line the median. B. The number of mapped bases did not correlate with the number of detected mutations in CD8+ cells (Spearman correlation), although a statistically significant correlation existed in CD4+ cells (Spearman correlation p= 0.02955).

**Supplementary Figure S4. Vertical and horizontal coverage of the custom gene sequencing panel.**

**A**



**B**

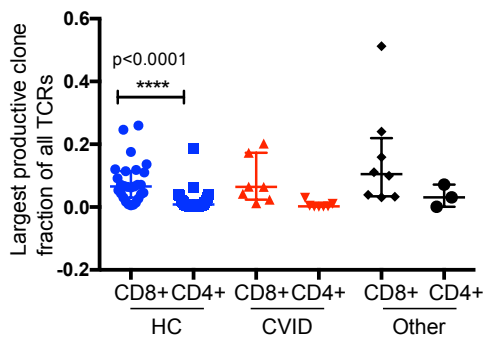


The percentage of bases covered by the given number (or more) of sequencing reads, presented as cumulative percentage. Colors show the depth. A. Coverages over the custom, targeted gene panel positions. B Coverages over all RefSeq genes. Abbreviations: DP, depth (the number of reads)

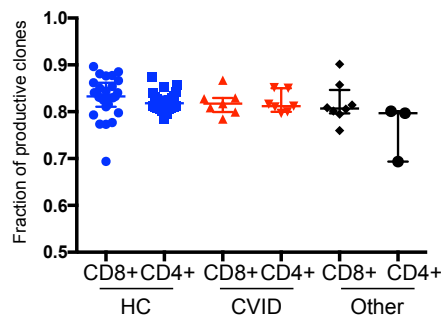


**Supplementary Figure S5. The largest clones and fraction of productive sequences in the sample.**

**A**

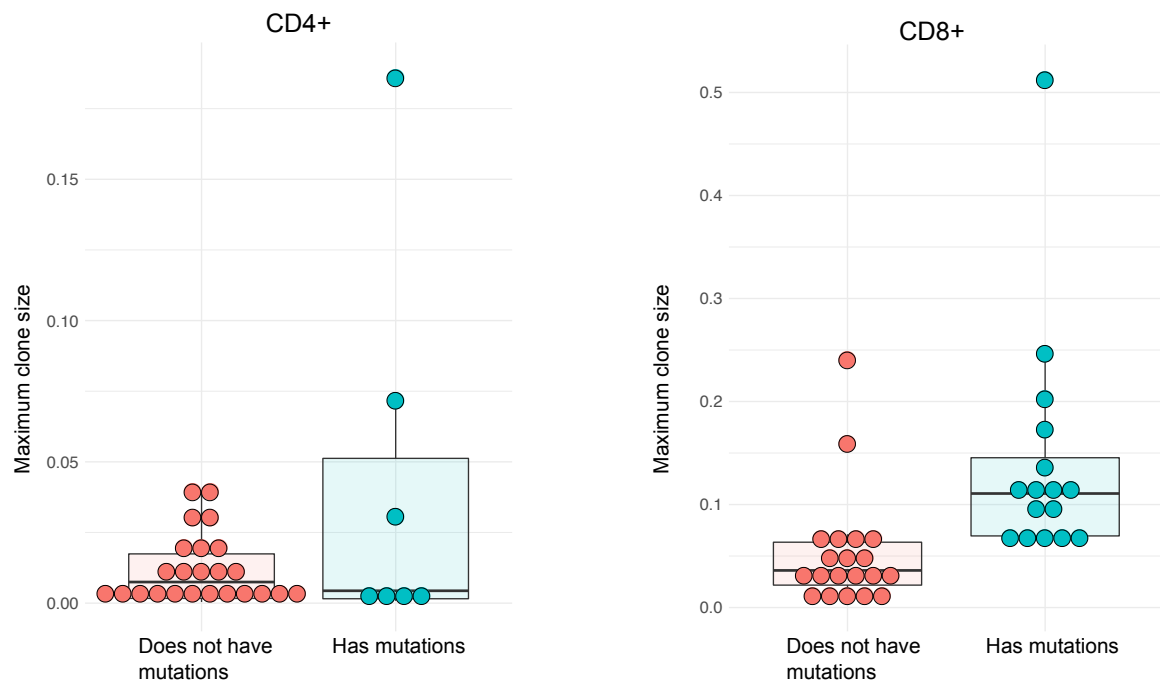


**B**



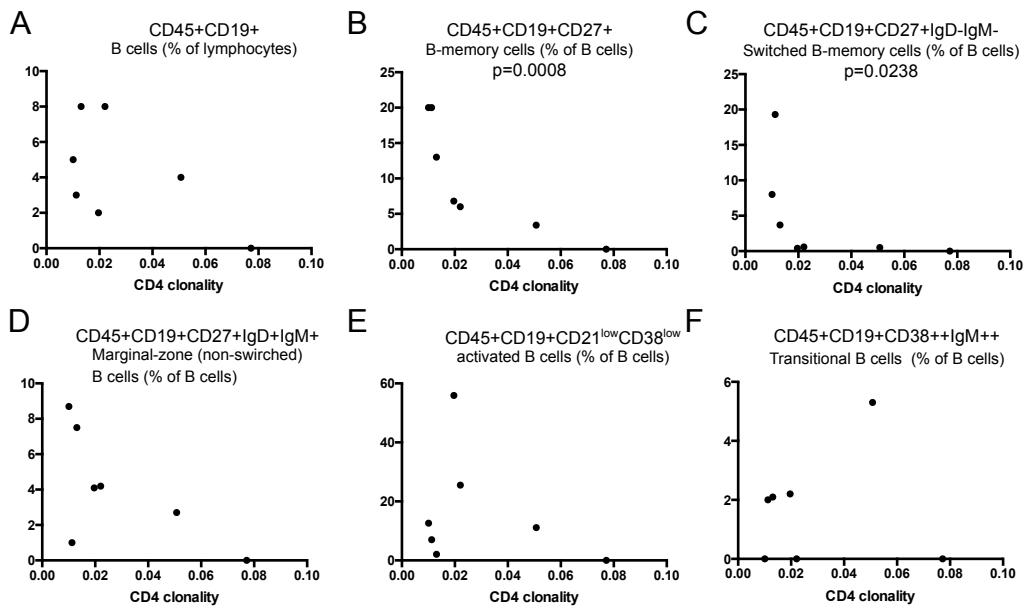
A. The largest clone (as frequency of all TCRB rearrangements in the sample) for each patient is shown. B. The fraction of productive TCRB rearrangements in the sample (frequency). Statistical tests comprised of Kruskal-Wallis test as an omnibus test and Dunn's multiple comparison tests as post-hoc tests. Statistically significant results are marked in the figure. The panels show group median, and error bars represent interquartile ranges.

### Supplementary Figure S6. Individuals with mutations have larges T-cell clones.



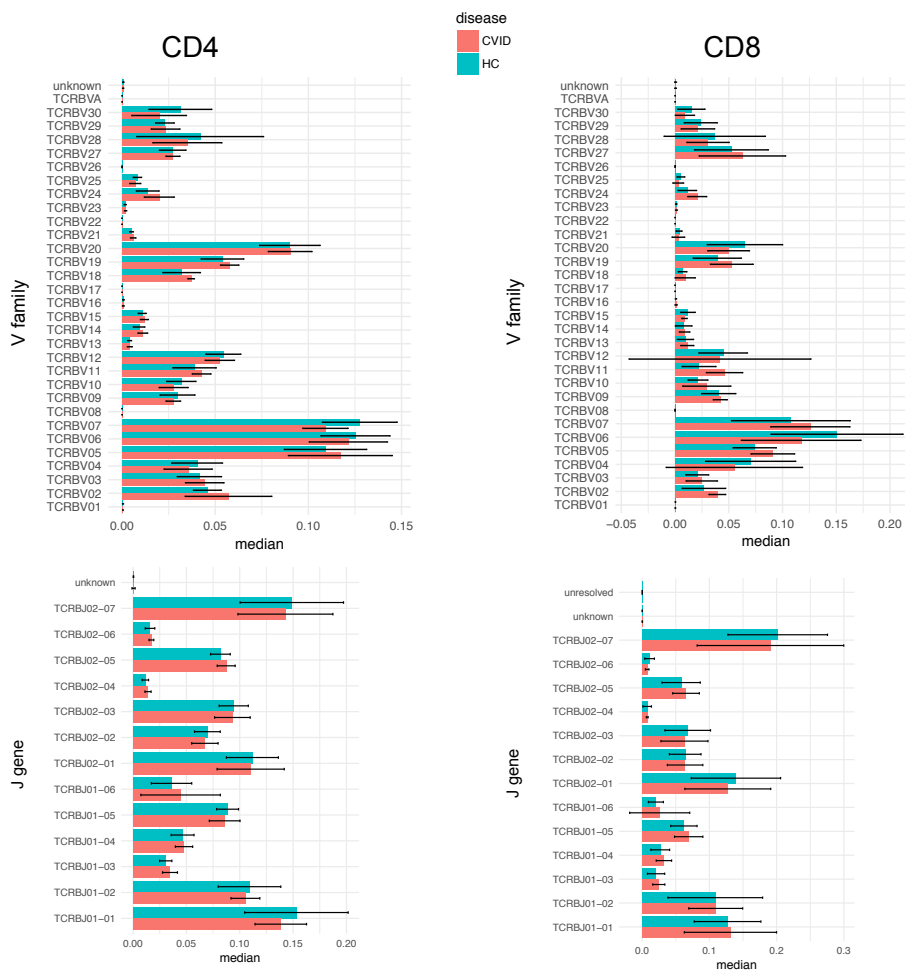
All individuals (both healthy controls and patients) were grouped using the existence of somatic mutations as a grouping factor. The sizes (frequency of all TCR rearrangements in the sample) of the largest T-cell clone in the sample were compared. In CD4+ cells, the clone sizes did not differ, but in CD8+ cells, individuals with mutations had larger T-cell clones (Mann-Whitney test  $p=4.991e-05$ ). Vertical lines in the plot represent the median, boxplot hinges interquartile ranges and whiskers reasonable extremes of the data.

**Supplementary Figure S7. CD4+ clonality correlations with B-cell subtype frequencies.**



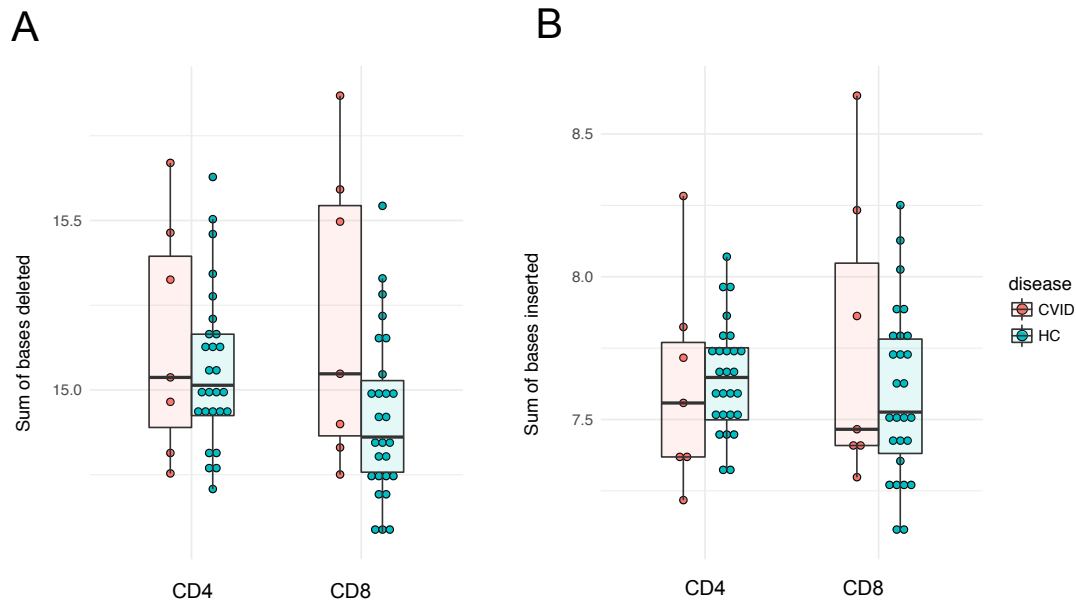
CD4+ clonality in CVID patients was plotted and correlated with the frequency of different B-cell subsets. Statistically significant correlations existed between B-memory and switched B-memory cells (Spearman correlation  $p=0.0008$  and  $p=0.0238$ ), but the associations were not linear.

### Supplementary Figure S8. V-family and J-gene usage in CVID patients and controls.



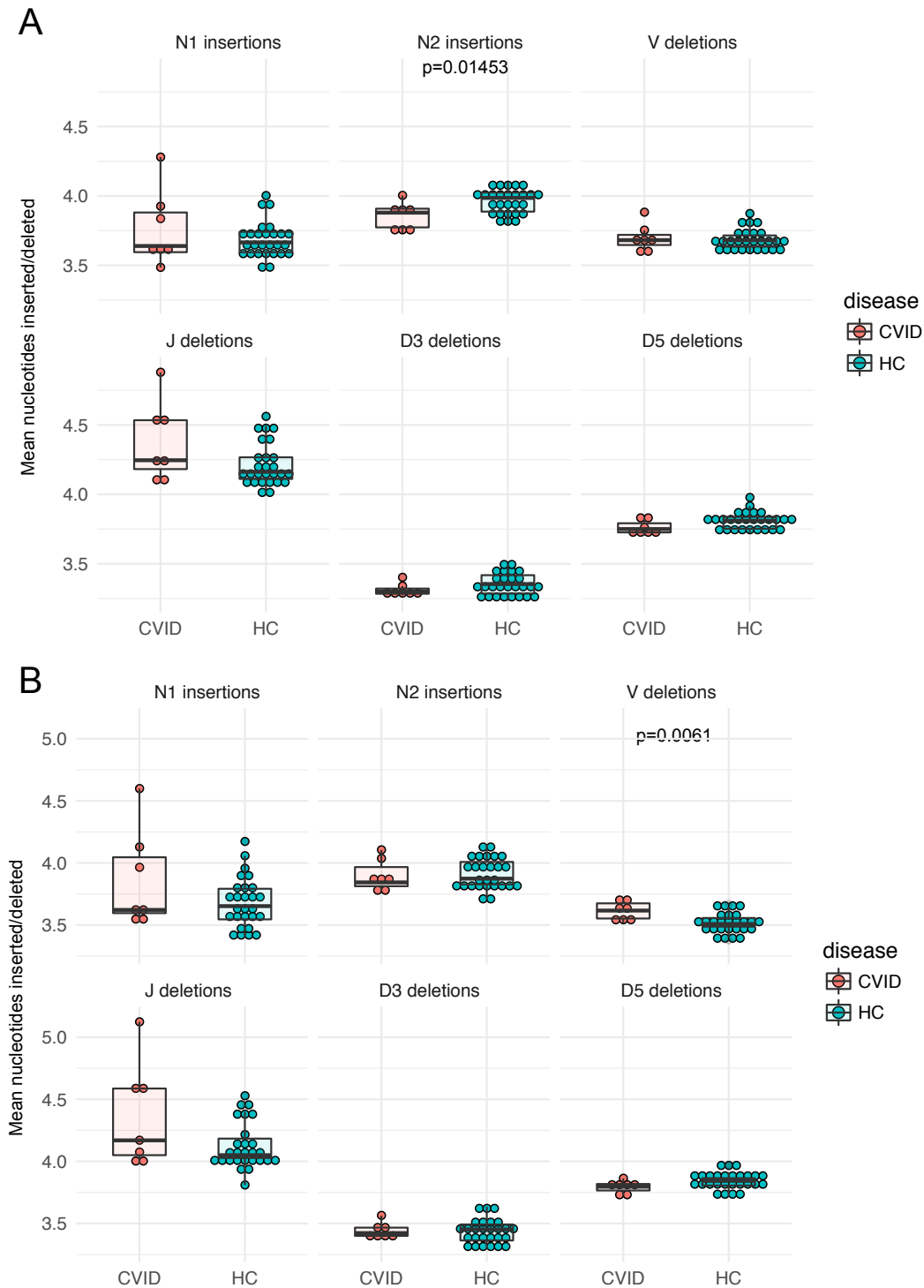
For each individual, the abundance of all TCRs that were classified to different V-families and J-genes were calculated. The graphs show the medians for CVID patients and healthy controls, and error bars represent interquartile ranges. No statistically significant differences were observed between patients and controls in neither V-family nor J-gene usage (Mann-Whitney test for each V-family and J-gene; p-values corrected for multiple comparisons with the Benjamini-Hochberg method).

**Supplementary Figure S9. CVID patients do not have more n-insertions or deletions than controls.**



The mean number of deletions (A) and non-templated insertions (B) was calculated for each individual and compared between controls and CVID patients. No statistically significant differences (Mann-Whitney test) existed between CVID patients and healthy controls. In the figure, medians, interquartile ranges, and reasonable extremes of the data are shown. Abbreviations: HC, healthy control; CVID, common variable immunodeficiency.

**Supplementary Figure S10. All base editions in CVID and HC TCRs.**

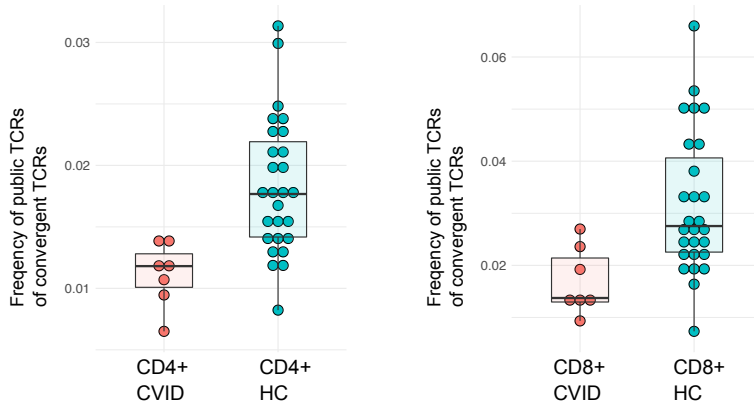


The mean number of base deletions and insertions are shown for CD4+ (A) and CD8+ cells (B). Medians, interquartile ranges, and reasonable extremes of the data are also shown. In most cases, no statistically significant differences occurred between CVID and healthy controls, but CVID CD4+ cells may have less N2 insertions and CVID CD8+ cells more V deletions than in healthy controls (Mann-Whitney test). Tests were not corrected for multiple comparisons, and thus caution in

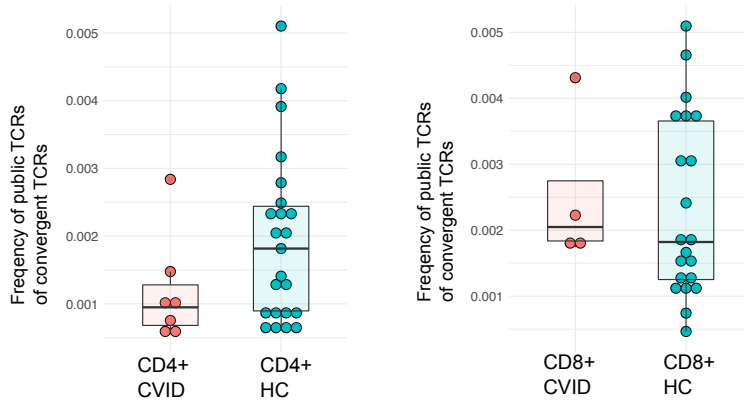
interpretation is needed. Abbreviations: HC, healthy control; CVID, common variable immunodeficiency.

**Supplementary Figure S11. Healthy controls show higher frequencies of public, pathogen-specific TCRs in their convergent TCRs than CVID patients.**

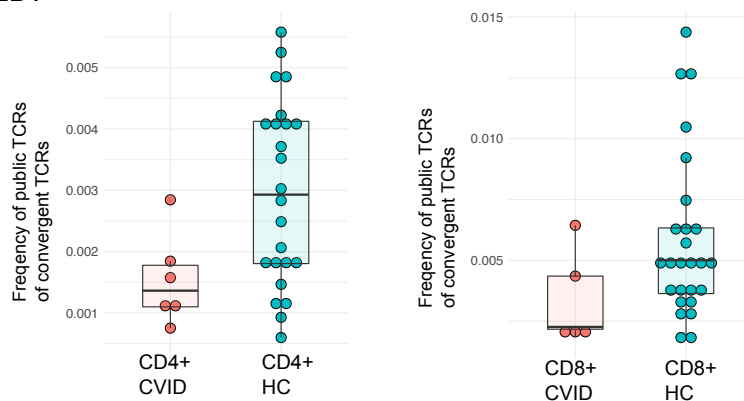
**A. All pathogens in the McPAS database**



**B. CMV**



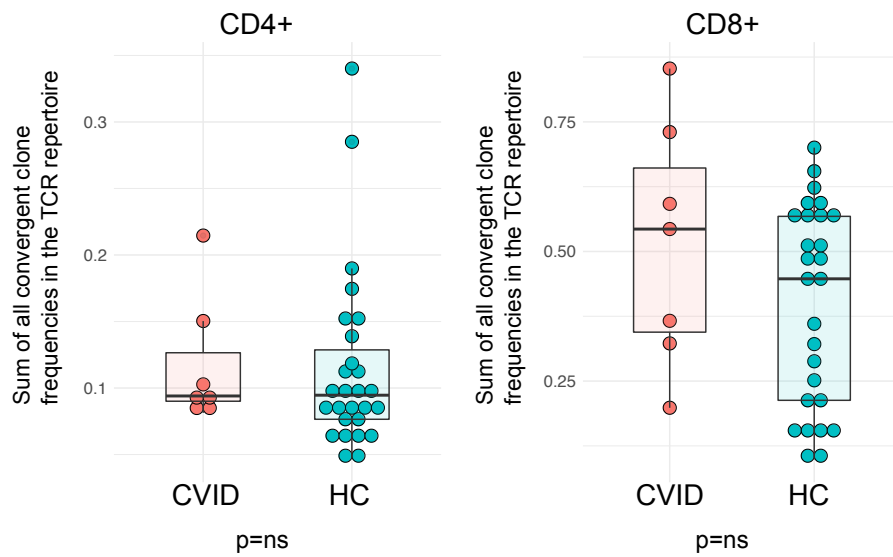
**C. EBV**



Frequency of public pathogen-specific TCRs of all convergent TCRs in both CVID patients' and healthy controls' CD4+ and CD8+ cells. Public pathogen-specific TCRs were extracted from the McPas database.<sup>10</sup> The pathogen-specific public TCRs comprised of TCRs targeting CMV, EBV, influenza, HIV, yellow fever virus, *Mycobacterium tuberculosis*, Herpes simplex 2 virus, and hepatitis C virus. Healthy controls harbored higher frequencies of public pathogen-specific TCRs in their repertoire of convergent TCRs (Mann-Whitney test  $p=0.0003454$  for CD4+;  $p=0.003182$  for CD8+) and EBV-specific CD4+ cells ( $p=0.03312$ ). The plots show median as a vertical line, and boxplot hinges represent interquartile ranges and whiskers reasonable extremes of the data.

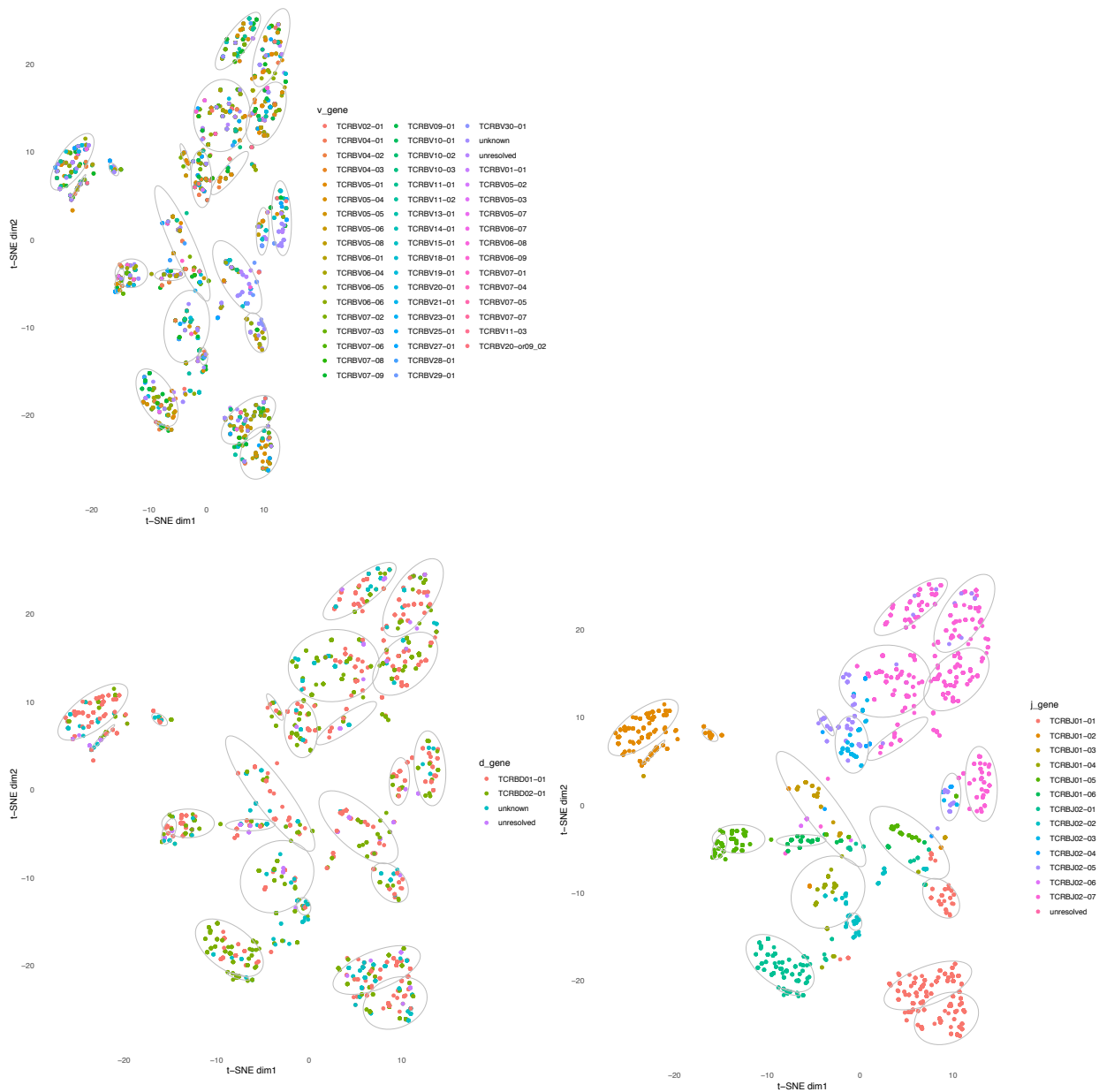


### Supplementary Figure S12. Abundance of convergent clones.



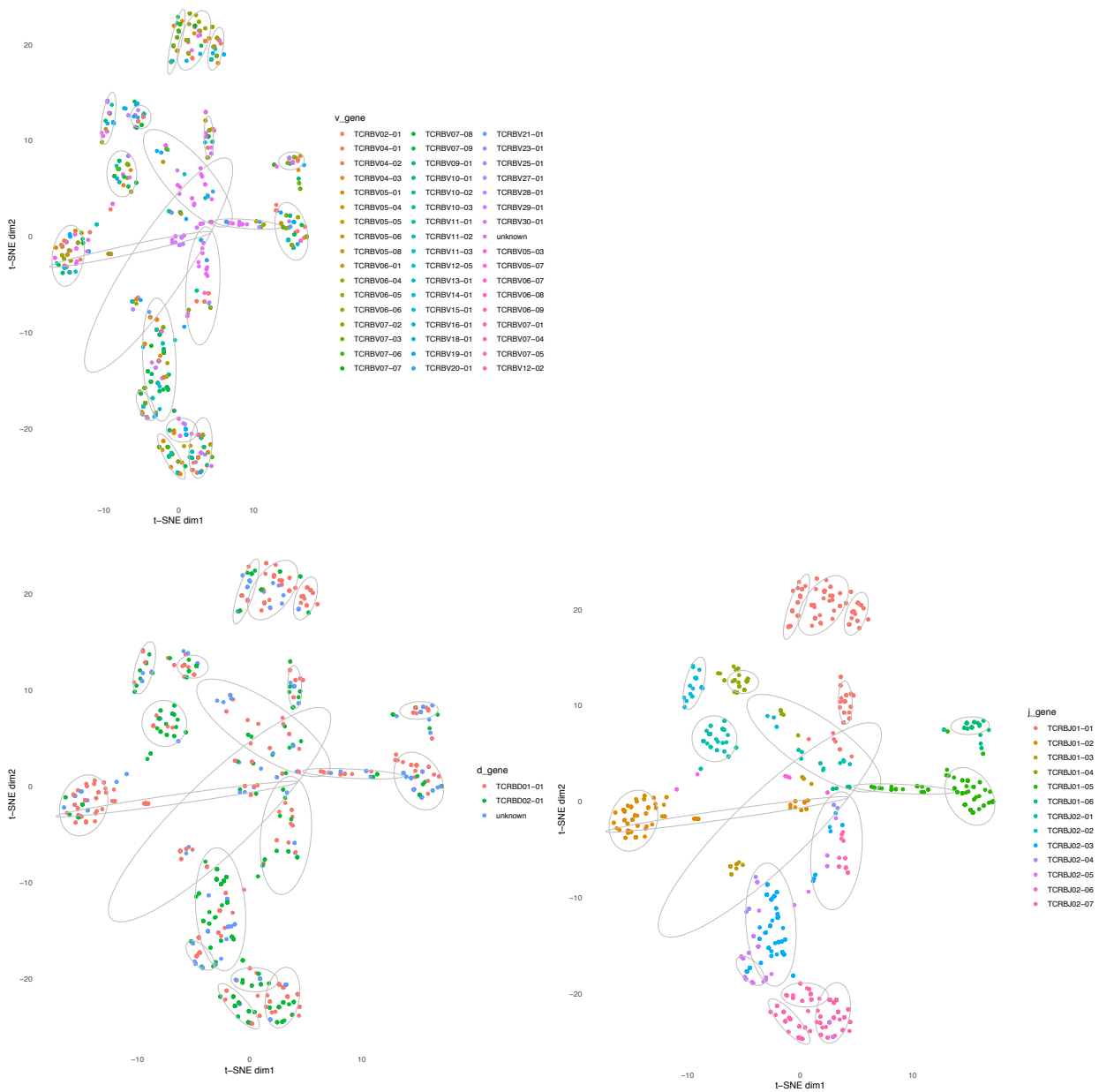
CVID patients did not show higher abundance (=sum of the frequencies of all rearrangements showing convergence) of convergent TCRs (Mann-Whitney test  $p = ns$  for CD4+ and CD8+). In the plots, vertical lines represent the median, box hinges interquartile ranges, and whiskers reasonable extremes of the data. Abbreviations: ns, not significant; HC, healthy control; CVID, common variable immunodeficiency.

**Supplementary Figure S13. VDJ gene usage mapped to CD8+ TCR clustering analysis.**



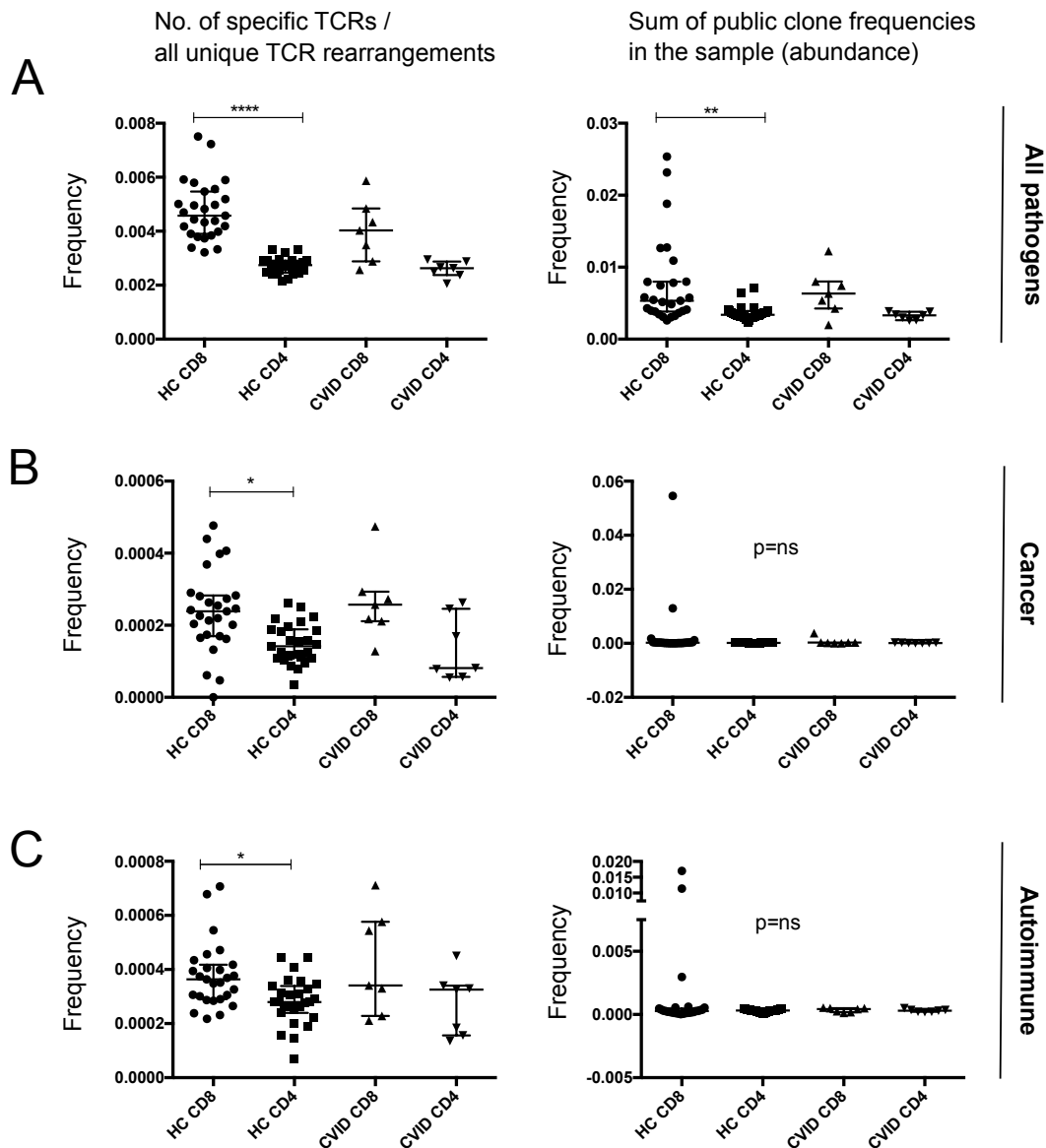
Physiochemical similarity analysis of selected CD8+ TCR CDR3 sequences by the GSKernel algorithm, presented as tSNE plots. TCRs are colored by their V-gene, D-gene, and J-genes. The V-gene does not clearly correlate with TCR similarity clusters, but the J-genes do. However, J-genes define a larger proportion of the TCR CDR3 than V- or D genes.

**Supplementary Figure S14. VDJ gene usage mapped to CD4+ TCR clustering analysis.**



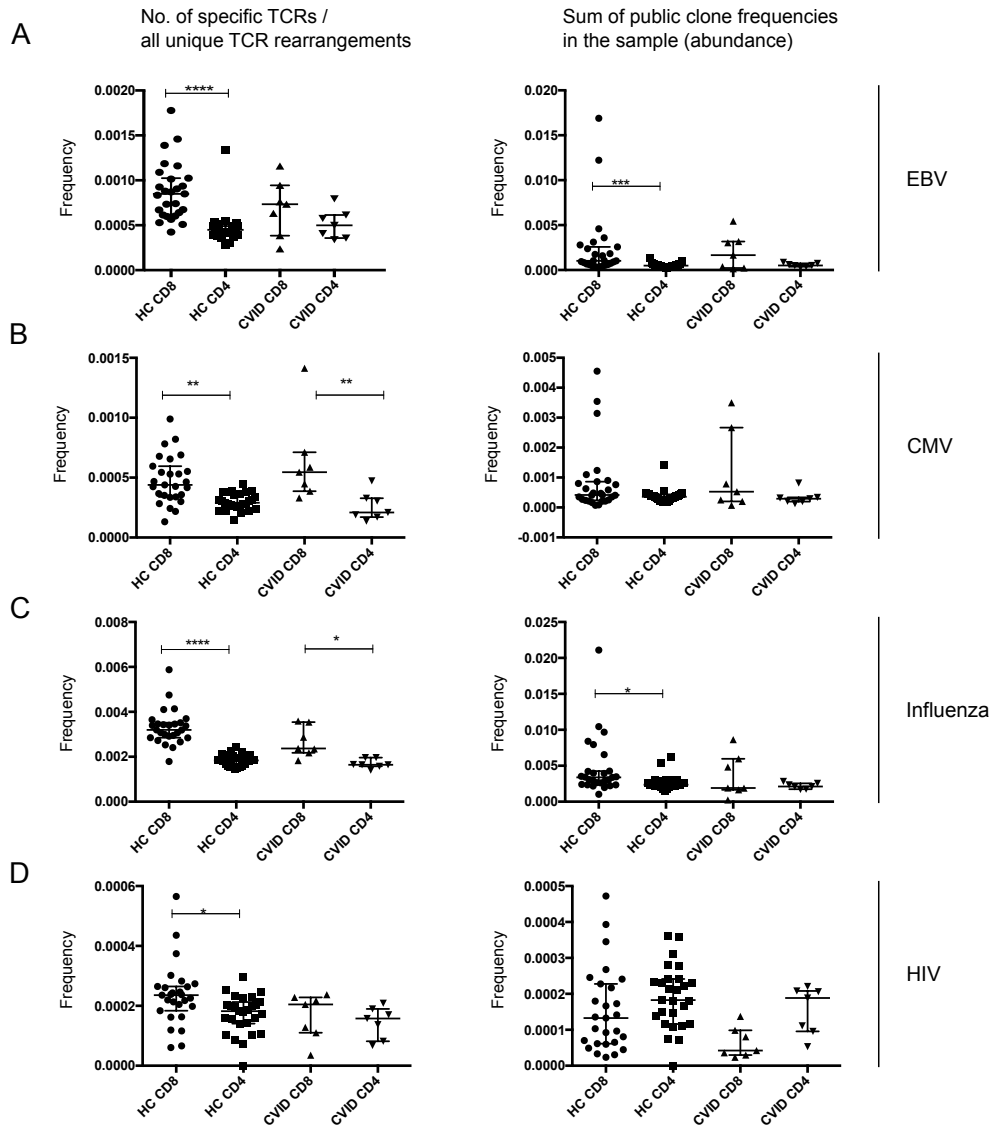
Physiochemical similarity analysis of selected CD4+ TCR CDR3 sequences by the GSKernel algorithm, presented as tSNE plots. TCRs are colored by their V-gene, D-gene, and J-genes. The V-gene does not clearly correlate with TCR similarity clusters, but the J-genes do. However, J-genes define a larger proportion of the TCR CDR3 than V- or D genes.

**Supplementary Figure S15. Pathogen-specific TCRs are more common in CD8+ cells than in CD4+ cells.**



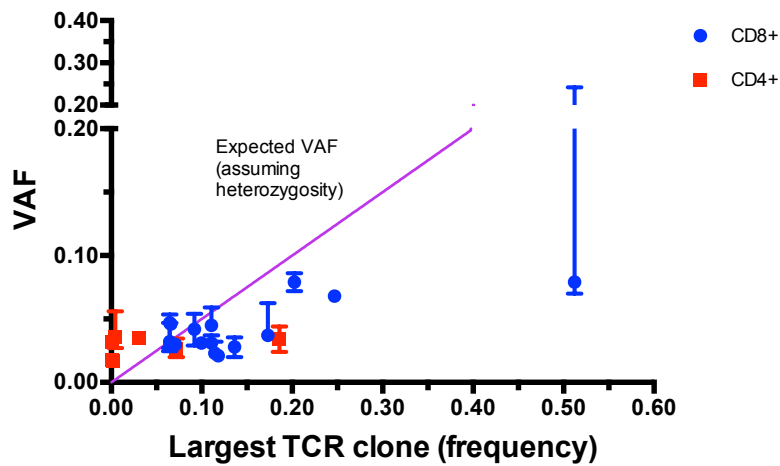
TCRB sequencing data was queried for matches for public, previously reported TCR sequences included in the McPAS database. The numbers of all pathogen-, cancer-, or autoimmune-associated TCRs were pooled for each patient and normalized for repertoire size. For pathogen- and cancer-associated TCRs, only antigen-specific TCRs were queried (labels “1” and “2” in the McPAS database), but for autoimmune TCRs, all autoimmune-associated TCRs were included in the analyses. Statistical tests comprised of Kruskal-Wallis test with Dunn’s multiple comparison tests. Panels A-C show the median and error bars represent interquartile ranges. Statistically significant results between comparisons (HC CD8+ vs HC CD4+, CVID CD8+ vs CD4+, CVID CD8+ vs HC CD8+, and CVID CD4+ vs HC CD4+) are shown. Abbreviations: ns, not significant; HC, healthy control; CVID, common variable immunodeficiency. \* $p < 0.05$ ; \*\* $p < 0.01$ ; \*\*\* $p < 0.001$ ; \*\*\*\* $p < 0.0001$ .

**Supplementary Figure S16. Virus-specific TCRs are more frequent in CD8+ cells than in CD4+ cells.**



TCRB sequencing data was queried for matches for public, previously reported TCR sequences included in the McPas database. Results for CMV, EBV, influenza, and HIV are shown. Only antigen-specific TCRs were queried (labels “1” and “2” in the McPAS database). Statistical tests comprised of Kruskal-Wallis test with Dunn’s multiple comparison tests. Panels A-D show the median and error bars represent interquartile ranges. Statistically significant results between comparisons (HC CD8+ vs HC CD4+, CVID CD8+ vs CD4+, CVID CD8+ vs HC CD8+, and CVID CD4+ vs HC CD4+) are shown. Abbreviations: HC, healthy control; CVID, common variable immunodeficiency. \* $p < 0.05$ ; \*\* $p < 0.01$ ; \*\*\* $p < 0.001$ ; \*\*\*\* $p < 0.0001$ .

### Supplementary Figure S17. T-cell clone size compared to variant-allele frequencies (VAFs)



For each patient, the median VAF of somatic mutations was plotted against the frequency of the largest T-cell clone in the same cell fraction of the same patient. Results for CD4+ and CD8+ cells are shown separately. The error bars represent interquartile range of the mutation VAFs in the patient. The purple line represents expected results, if (1) all mutations were heterozygous, (2) they occurred in the largest T-cell clone, and (3) they existed in all cells of that largest clone. The results from CD8+ cells were as expected and in line with our previous results.<sup>37</sup> However, some CD4+ cells harbor mutations with large VAFs compared to clone sizes.

## References

1. Selenius JS, Martelius T, Pikkarainen S, et al. Unexpectedly high prevalence of common variable immunodeficiency in Finland. *Front Immunol* 2017;8:1190.
2. Trotta L, Martelius T, Siitonen T, et al. ADA2 deficiency: Clonal lymphoproliferation in a subset of patients. *J Allergy Clin Immunol* 2018;141(4):1534–1537.
3. Haapaniemi EM, Kaustio M, Rajala HLM, et al. Autoimmunity, hypogammaglobulinemia, lymphoproliferation, and mycobacterial disease in patients with activating mutations in STAT3. *Blood* 2015;125(4):639–649.
4. Seppänen M, Koillinen H, Mustjoki S, Tomi M, Sullivan KE. Terminal deletion of 11q with significant late-onset combined immune deficiency. *J Clin Immunol* 2014;34(1):114–118.
5. Wehr C, Kivioja T, Schmitt C, et al. The EUROclass trial : defining subgroups in common variable immunodeficiency. *Blood* 2008;111(1):77–85.
6. Warnatz K, Denz A, Dra R, et al. Severe deficiency of switched memory B cells ( CD27+1 IgM- IgD-) in subgroups of patients with common variable immunodeficiency : a new approach to classify a heterogeneous disease. *Blood* 2002;99(5):1544–1552.
7. Morgan AW, Thomson W, Martin SG, et al. Reevaluation of the interaction between HLA-DRB1 shared epitope alleles, PTPN22, and smoking in determining susceptibility to autoantibody-positive and autoantibody-negative rheumatoid arthritis in a large UK caucasian population. *Arthritis Rheum* 2009;60(9):2565–2576.
8. Carlson CS, Emerson RO, Sherwood AM, et al. Using synthetic templates to design an unbiased multiplex PCR assay. *Nat Commun* 2013;4:2680.
9. Robins HS, Campregher P V, Srivastava SK, et al. Comprehensive assessment of T-cell receptor beta-chain diversity in alphabeta T cells. *Blood* 2009;114(19):4099–4107.
10. Tickotsky N, Sagiv T, Prilusky J, Shifrut E, Friedman N. McPAS-TCR: A manually curated catalogue of pathology-associated T cell receptor sequences. *Bioinformatics* 2017;33(18):2924–2929.
11. Giguère S, Marchand M, Laviolette F, Drouin A, Corbeil J. Learning a peptide-protein binding affinity predictor with kernel ridge regression. *BMC Bioinformatics* 2013;14(1):82.
12. Levine JH, Simonds EF, Bendall SC, et al. Data-Driven Phenotypic Dissection of AML Reveals Progenitor-like Cells that Correlate with Prognosis. *Cell* 2015;162(1):184–197.
13. Van Der Maaten LJP, Hinton GE. Visualizing high-dimensional data using t-SNE. *J Mach Learn Res* 2008;(9):2579–2605.
14. Cruciani G, Baroni M, Carosati E, Clementi M, Valigi R, Clementi S. Peptide studies by means of principal properties of amino acids derived from MIF descriptors. *J Chemom* 2004;18(34):146–155.
15. Breuer K, Foroushani AK, Laird MR, et al. InnateDB: Systems biology of innate immunity and beyond - Recent updates and continuing curation. *Nucleic Acids Res* 2013;41(Database issue):D1228–D1233.
16. Lynn DJ, Chan C, Naseer M, et al. Curating the innate immunity interactome. *BMC Syst Biol* 2010;4:117.
17. Lynn DJ, Winsor GL, Chan C, et al. InnateDB: Facilitating systems-level analyses of the mammalian innate immune response. *Mol Syst Biol* 2008;4:218.
18. Dufva O, Kankainen M, Kelkka T, et al. Aggressive natural killer-cell leukemia mutational landscape and drug profiling highlight JAK-STAT signaling as therapeutic target. *Nat Commun* 2018;9:1567.
19. Bolger AM, Lohse M, Usadel B. Trimmomatic: a flexible trimmer for Illumina sequence data. *Bioinformatics* 2014;30(15):2114–2120.
20. Li H. Aligning sequence reads, clone sequences and assembly contigs with BWA-MEM. Prepr [Epub ahead of print].
21. McKenna A, Hanna M, Banks E, et al. The Genome Analysis Toolkit: a MapReduce

- framework for analyzing next-generation DNA sequencing data. *Genome Res* 2010;20(9):1297–1303.
22. Cibulskis K, Lawrence MS, Carter SL, et al. Sensitive detection of somatic point mutations in impure and heterogeneous cancer samples. *Nature biotechnology* 2013;31(3):213–219.
  23. Zhao H, Sun Z, Wang J, Huang H, Kocher J-P, Wang L. CrossMap: a versatile tool for coordinate conversion between genome assemblies. *Bioinformatics* 2014;30(7):1006–1007.
  24. Wang K, Li M, Hakonarson H. ANNOVAR: functional annotation of genetic variants from high-throughput sequencing data. *Nucleic Acids Res* 2010;38(16):e164.
  25. Jaiswal S, Fontanillas P, Flannick J, et al. Age-related clonal hematopoiesis associated with adverse outcomes. *N Engl J Med* 2014;371(26):2488–98.
  26. Jaiswal S, Natarajan P, Silver AJ, et al. Clonal Hematopoiesis and Risk of Atherosclerotic Cardiovascular Disease. *N Engl J Med* 2017;377(2):111–121.
  27. Genovese G, Kähler AK, Handsaker RE, et al. Clonal Hematopoiesis and Blood-Cancer Risk Inferred from Blood DNA Sequence. *N Engl J Med* 2014;371(26):2477–2487.
  28. Fabregat A, Jupe S, Matthews L, et al. The Reactome Pathway Knowledgebase. *Nucleic Acids Res* 2018;46(D1):D649–D655.
  29. Ashburner M, Ball CA, Blake JA, et al. Gene ontology: tool for the unification of biology. The Gene Ontology Consortium. *Nat Genet* 2000;25(1):25–29.
  30. Expansion of the Gene Ontology knowledgebase and resources. *Nucleic Acids Res* 2017;45(D1):D331–D338.
  31. Rosenthal R, McGranahan N, Herrero J, Taylor BS, Swanton C. deconstructSigs: delineating mutational processes in single tumors distinguishes DNA repair deficiencies and patterns of carcinoma evolution. *Genome Biol* 2016;17(1):31.
  32. Alexandrov LB, Nik-Zainal S, Wedge DC, et al. Signatures of mutational processes in human cancer. *Nature* 2013;500(7463):415–421.
  33. Savola P, Lundgren S, Keränen MAI, et al. Clonal hematopoiesis in patients with rheumatoid arthritis. *Blood Cancer J* 2018;8(8):69.
  34. Dobin A, Davis CA, Schlesinger F, et al. STAR: ultrafast universal RNA-seq aligner. *Bioinformatics* 2013;29(1):15–21.
  35. Liao Y, Smyth GK, Shi W. The Subread aligner: fast, accurate and scalable read mapping by seed-and-vote. *Nucleic Acids Res* 2013;41(10):e108.
  36. Robinson MD, McCarthy DJ, Smyth GK. edgeR: a Bioconductor package for differential expression analysis of digital gene expression data. *Bioinformatics* 2010;26(1):139–140.
  37. Savola P, Kelkka T, Rajala HLM, et al. Somatic mutations in clonally expanded cytotoxic T lymphocytes in patients with newly diagnosed rheumatoid arthritis. *Nat Commun* 2017;8:15869.